

LaTeX Diff

Old: template.tex New: template_Rev2.tex

~~Deleted text~~ Added text Unchanged text

--- template.tex

+++ template_Rev2.tex

```
@@ -78,9 +78,11 @@
```

```
%\usepackage{subfig}
%\usepackage{rotating}
\usepackage{setspace}
\doublespacing
\usepackage{wasysym}
\usepackage{footmisc}
\begin{document}
```

```
\title{An Order of Magnitude Signal-to-Noise Improvement of Magnetic Resonance Spectra using a
Segmented-Overlap Fourier-Filtering and Averaging (SOFFA) Approach.}
\title{Signal-to-Noise Improvement of Magnetic Resonance Spectra using a Segmented-Overlap Fourier-Filtering
and Averaging (SOFFA) Approach.}
```

```
@@ -103,7 +105,7 @@
```

```
\runningtitle{TBXT}
\runningauthor{TBXT}
\runningtitle{Signal-to-Noise Improvement of Magnetic Resonance Spectra using a Segmented-Overlap
Fourier-Filtering and Averaging (SOFFA) Approach.}
\runningauthor{Jason W. Sidabras}
```

```
@@ -127,5 +129,5 @@
```

```
\begin{abstract}
```

Segmented-Overlap Fourier-Filtering and Averaging (SOFFA) data acquisition method is described in detail for magnetic resonance spectroscopy. In this work the four processes that encompass the SOFFA data acquisition method are detailed: (i) oversampling spectral segments, (ii) Fourier block-filtering, (iii) segment-overlap averaging, and (iv) decimation. Three experimental examples are ~~shown. Conventional Continuous Wave (CW) Electron Paramagnetic Resonance (EPR) is compared to SOFFA-CW of a single reduced [4Fe-4S]^{S=1/2} at concentrations of 1~mM, 100~ μ M, and 10~ μ M showing an average increase in concentration sensitivity by a factor of 5.6. Experimental comparison of CW and SOFFA non-adiabatic rapid scan (SOFFA-NARS) data with similar filter parameters and field-modulation amplitude demonstrates a factor of 10.3 in signal-to-noise improvement for a 150~ μ M site-directed spin-labeled Hemoglobin in 82% glycerol at 18 $^{\circ}$ C. The signal-to-noise improvements were made for the same data acquisition times on standard commercial instruments. This method can be implemented to perform real-time segmented processing and, combined with more sophisticated averaging methods, will push the state-of-the-art sensitivity in magnetic resonance spectroscopy.~~

Segmented-Overlap Fourier-Filtering and Averaging (SOFFA) data acquisition method is described in detail for magnetic resonance spectroscopy. In this work the four processes that encompass the SOFFA data acquisition method are detailed: (i) oversampling spectral segments, (ii) Fourier block-filtering, (iii) segment-overlap averaging, and (iv) decimation. Three experimental examples are **shown: First, conventional continuous wave (CW) electron paramagnetic resonance (EPR) is compared to SOFFA-CW of a single reduced [4Fe-4S]^{S=1/2} at concentrations of 1~mM, 100~ μ M, and 10~ μ M showing an average increase in concentration sensitivity by a factor of 5.6 in 100 minute measurement time. Second, an experimental comparison of CW and SOFFA non-adiabatic rapid scan (SOFFA-NARS) data with similar filter parameters and field-modulation amplitude demonstrates a factor of 10.3 in signal-to-noise improvement (32 minute measurement time) for a 150~ μ M site-directed spin-labeled Hemoglobin in 82% glycerol at 18 $^{\circ}$ C. Finally, a signal-to-noise matched experiment of free TEMPO at 10~ μ M concentration is presented, where CW was performed at 400 scans (273 minutes) compared to SOFFA-CW with an overlap factor of 100 (20 minutes). Also shown is the effect of 1/f noise on these CW and SOFFA-CW experiments. Ultimately, the SOFFA algorithm achieves sensitivity enhancement by combining massive digital oversampling and out-of-band noise filtration with coherent spatial accumulation of highly overlapped spectral segments. The gains reported here are phenomenological and are grounded in established DSP principles but validated through experiment rather than closed-form analytical prediction. This fundamental restructuring of the acquisition chain successfully decouples high-frequency filtering from low-frequency averaging, while providing a data collection scheme that suppresses 1/f noise. The SOFFA method can be implemented to perform real-time segmented processing and, combined with more sophisticated averaging methods, will push the state-of-the-art sensitivity in magnetic resonance spectroscopy.**

\end{abstract}

@@ -135,103 +137,119 @@

\introduction %% \introduction[modified heading if necessary]

~~In this work, the Segmented-Overlap Fourier Filtering and Averaging (SOFFA) method for magnetic resonance data acquisition and filtering is established. In a typical continuous-wave (CW) Electron Paramagnetic Resonance (EPR) experiment a spectrum is collected as a continuous signal, \textit{i.e.} the spectroscopist must ``play'' it until the end and, only then, repeat for averaging. However, the signal is typically time invariant, and therefore can be collected in a number of unique ways. It is shown herein that by collecting a magnetic resonance spectrum in segments an additional parameter related to the overlap of each scan is introduced. Each acquired segment contains field- or frequency-stepped correlated signal and uncorrelated noise. For processing, each segment is oversampled, filtered block-wise, and concatenated resulting in a signal-to-noise improvement compared to traditional CW and rapid scan data collection, averaging, and filtering methods for the same measurement time. The SOFFA data acquisition method can be adopted for many magnetic resonance experiments and is demonstrated for conventional CW and rapid scan techniques. The scheme is illustrated in Fig. \ref{fig:overlap-add-filt}.~~

~~\begin{figure}[htbp]~~

In this work, the Segmented-Overlap Fourier Filtering and Averaging (SOFFA) method for magnetic resonance data acquisition and filtering is established. In a typical continuous-wave (CW) Electron Paramagnetic Resonance (EPR) experiment a spectrum is collected as a continuous signal, \textit{i.e.} the spectroscopist must ``play'' it until the end and, only then, repeat for averaging. However, the signal is typically time invariant, and therefore can be collected in a number of unique ways. It is shown herein that by collecting a magnetic resonance spectrum in segments an additional parameter related to the overlap of each scan is introduced, while increasing the available number of data points collected. Each acquired segment contains field- or frequency-stepped correlated signal and uncorrelated noise. For processing, each segment is oversampled, filtered block-wise, concatenated, and decimated to a standard number of points (i.e. 1024) resulting in a signal-to-noise improvement compared to traditional CW or non-adiabatic rapid scan (NARS) data collection, averaging, and filtering methods for the same measurement time. The SOFFA data acquisition method can be adopted for many magnetic resonance experiments and is demonstrated for conventional CW and NARS techniques. A visualization of the scheme is illustrated in Fig.~\ref{fig:test-data}.

\begin{figure}[htb]

\begin{center}

~~\includegraphics[height=0.85\textheight]{01-overlapadd-filter.eps}~~

~~\caption{Illustration of the SOFFA data acquisition method used to concatenate and filter segmented magnetic resonance data. Herein, the filter $S_{\text{H}}[\omega]$ is a Gaussian in the frequency domain. The discrete indices of the collected segments $\{k\}$ and the final concatenated output $y_{\text{tot}}[i]$ map directly to the physical sweep axis (e.g., mT for field sweeps or MHz for frequency sweeps).}~~

~~\label{fig:overlap-add-filt}~~

\includegraphics{03a-TestData.eps}

\caption{A visualization of the SOFFA method. A Gaussian absorption spectrum is simulated with a half width of 1 mT and an amplitude of unity. Shown here is a representation of the simulated experiment. (A) Random (white) noise is added. (B) Small set of unfiltered segmented data is plotted showing field steps δs with oversampling. Illustration of segmentation is shown in the inset over length L . (C) When a Gaussian convolution filter of Eq. \ref{eq:filter} is applied to $\{A\}$, the expected improvement in signal-to-noise is shown, similar to increasing the time constant. (D) However, using the SOFFA method, as L is increased, further signal-to-noise improvement is exhibited due to the increased averaging during concatenation of filtered data.}

\label{fig:test-data}

\end{center}

\end{figure}

~~The improved signal to noise ratio (SNR) achieved by the SOFFA method can also be leveraged to reduce the time required for an experiment, thereby increasing throughput. In traditional EPR experiments, the SNR is often improved by averaging multiple scans, which can be time consuming. However, with the SOFFA method, the same level of SNR can be achieved in a shorter amount of time, typically by the square of the number of traditional averages. This means that the experiment time can be reduced, allowing for more samples to be analyzed in a given time period. By using the SOFFA method, this relationship can be decoupled, allowing for improved SNR without a corresponding increase in experiment time. This can have significant implications for high throughput applications, such as screening large numbers of samples or performing kinetic studies. The non-adiabatic rapid scan (NARS) \citep{KITTELL2011220, KITTELL201251, KITTELL201568, HYDE201315, YU201558} method collect pure absorption EPR spectra using fast field or frequency sweeps and modern digital signal processing. Both rapid scan methods collect quadrature pure absorption EPR spectra, which can be pseudo modulated to the conventional first derivative EPR spectrum. \citep{Hyde1990, HYDE201315} In a NARS experiment, the field or frequency is swept at a rate and amplitude that allows the spin system to return to thermal equilibrium and no passage is observed. In this sense, NARS mimics a CW EPR experiment and the power saturation profile of the sample remains unperturbed. Typically, NARS experiments employ low amplitude (1 mT) and rate (below 50 kHz) for field or frequency sweeps. In order to collect a full EPR spectrum, the static field is stepped and data are collected. Each step is windowed, zero filled, concatenated, and filtered. The advantage of NARS comes from the modern data collection methods (averaging, digital filtering, etc.), collection of pure absorption spectra, and signal to noise improvements due to overlapping segments during concatenation. NARS has been used by Hyde and colleagues \citep{KITTELL2011220, KITTELL201568} at L-band (1.2 GHz) to extend the deconvolution method of CW EPR distance determination from~~

~~18-25-AA{} to 30-35-AA{} \citep{KITTELL201251} and increase the resolution for a copper imidazole complex. \citep{HYDE201315} Additionally, NARS was independently shown by Eaton and colleagues in applications of spectra as wide as 620-mT. \citep{YU201558} It has been established that non-adiabatic rapid scan data collection produces a comb filter that suppresses high frequency noise. \citep{Wilmshurst, misraRS} However, these methods are susceptible to low frequency noise that is correlated with the field sweep or the transfer function of the frequency response of the system. Filtering such noise is problematic since the features may contain the same frequency content as the absorption spectrum. For instance, pseudo-modulation using the Moving Difference (MDIFF) algorithm to calculate the conventional first harmonic derivative like spectrum further reduces some low frequency noise. \citep{HYDE201315} However, the challenge of properly filtering NARS data still remains. The SOFFA data acquisition method is shown to remove challenging noise profiles and that the method is well suited for magnetic resonance spectroscopy with minimum changes to data acquisition. The SOFFA data acquisition method is tested with (i) an experimental comparison between an averaged and filtered CW spectrum and a SOFFA CW spectrum using concentrations of 1-mM, 100- μM , and 10- μM of \textit{apo} [FeFe] hydrogenase (single reduced [4Fe-4S]⁺; S=1/2; Ref. \citep{Knorzer06012012}), (ii) an experimental comparison of a SOFFA NARS spectrum of 150- μM site directed spin labeled Hemoglobin protein in 82% glycerol at 18 $^{\circ}\text{C}$ to averaged and filtered CW spectrum, and (iii) an experimental comparison between traditional and SOFFA RS spectra of a minuscule amount of lithium phthalocyanine (LiPC). For direct comparison the measurement time was kept constant for each set of experiments.~~

The improved signal-to-noise ratio (SNR) achieved by the SOFFA method can also be leveraged to reduce the time required for an experiment, thereby increasing throughput. In traditional EPR experiments, the SNR is often improved by averaging multiple scans, which can be time-consuming. However, with the SOFFA method, the same level of SNR can be achieved in a shorter amount of time, typically by the square of the number of traditional averages. This means that the experiment time can be reduced, allowing for more samples to be analyzed in a given time period. By using the SOFFA method, this relationship can be decoupled, allowing for improved SNR without a corresponding increase in experiment time.

The limitations of the SOFFA-CW method are primarily twofold: The first is practical step sizes of commercial magnets are limited to 0.01-mT steps. This is due to both the settling time of a magnet and the hysteresis associated with a large electromagnet returning to a precision point before sweeping again. The second is the rate you can sweep through the spectrum, both from a physical constraint of the electromagnetic and to ensure that sweeping through the EPR line does not cause broadening from passage. \citep{Weger1960} These two practical limitations are largely eliminated using the non-adiabatic rapid scan (NARS) method. \citep{KITTELL2011228, KITTELL201251, KITTELL201568, HYDE201315, YU201558}

In a NARS experiment, the field or frequency is swept at a rate and amplitude that allows the spin system to return to thermal equilibrium and no passage is observed and the pure absorption lineshape is recorded. In this sense, NARS mimics a CW EPR experiment and the power saturation profile of the sample remains unperturbed. Typically, NARS experiments employ low amplitude (1-mT) and rate (below 50-kHz) for field or frequency sweeps. The increased rate and amplitude at a fixed field position of a NARS experiment generate harmonics which are captured completely with a digitizer. However, in order to collect a full EPR spectrum, the static field is stepped as opposed to swept like a traditional CW experiment. Each step is windowed, zero filled, concatenated, and filtered. The advantage of NARS comes from the modern data collection methods (averaging, digital filtering, etc.), collection of pure-absorption spectra, and signal-to-noise improvements due to overlapping segments during concatenation. The NARS method collects quadrature pure-absorption EPR spectra, which can be pseudo-modulated to the conventional first-derivative EPR spectrum. \citep{Hyde1990, HYDE201315} NARS has been used by Hyde and colleagues \citep{KITTELL2011228, KITTELL201568} at L-band (1.2-GHz) to extend the deconvolution method of CW EPR distance determination from 18-25-AA{} to 30-35-AA{} \citep{KITTELL201251} and used to increase the resolution for a copper imidazole complex. \citep{HYDE201315} Additionally, NARS was independently shown by Eaton and colleagues in applications of spectra as wide as 620-mT using concatenation without overlap. \citep{YU201558}

It has been established that NARS data collection produces a comb filter that suppresses high frequency noise. \citep{Wilmshurst, misraRS} However, these methods are susceptible to low frequency noise that is correlated with the field sweep or the transfer function of the frequency response of the system. Filtering such noise is problematic since the features may contain the same frequency content as the absorption spectrum. Pseudo-modulation using the Moving Difference (MDIFF) algorithm to calculate the conventional first-harmonic derivative-like spectrum further reduces some low frequency noise. \citep{HYDE201315} However, the challenge of properly filtering NARS data still remains. The SOFFA data acquisition method is shown to remove challenging noise profiles and that the method is well suited for magnetic resonance spectroscopy with minimum changes to data acquisition.

It should be noted that the signal-to-noise improvements reported herein are phenomenological in character. While the SOFFA method is constructed from well-established DSP principles (oversampling theory, Fourier block-filtering, and overlap-add averaging) a complete closed-form analytical expression that quantitatively predicts the net gain from the combination of all four processing stages is beyond the scope of this work. The experimental results serve as the primary validation. Future work will focus on a rigorous theoretical framework that decomposes the contributing factors and yields quantitative predictions as a function of acquisition parameters.

In this work, the SOFFA data acquisition method is tested with (i) an experimental comparison between an averaged and filtered CW spectrum and a SOFFA-CW spectrum using concentrations of 1-mM, 100- μM , and 10- μM of \textit{apo} [FeFe]-hydrogenase (single reduced [4Fe-4S]⁺; S=1/2; Ref. \citep{Knorzer06012012}), (ii) an experimental comparison of a SOFFA-NARS spectrum of 150- μM site-directed spin-labeled Hemoglobin protein in 82% glycerol at 18 $^{\circ}\text{C}$ to averaged and filtered CW spectrum. While (iii) an experimental comparison between CW and SOFFA-CW using a 10- μM TEMPO

(2,2,6,6-Tetramethylpiperidine-1-oxyl) radical in water where signal-to-noise is matched.

\section{Methods}

All data are processed using Wolfram Mathematica (v. 11.3; Champaign, IL, USA), where the SOFFA algorithm was implemented and validated across various experimental conditions. While Mathematica served as the primary engineering and development environment, a standalone Python-based GUI application has been provided to ensure the method is accessible and easily disseminated to the broader community. Data were collected on several spectrometers using the parameters specified for each case. To acquire segmented CW EPR spectra, a ProDEL program was developed for the Bruker Xepr environment, which automates discrete field stepping and lock-in detector data acquisition. \footnote{The ProDEL program and the Python GUI application can be found at <https://github.com/jsidabras/SOFFABruker>. \label{foot:github}} Each segment was stored in a 2D representation and saved in standard Bruker format (DSC/DTA). Little overhead was found using ProDEL programming up to 1200 segments (0.1 G steps over 120 G spectrum)

To ensure spectral fidelity, the magnetic field sweep rate for each segment must be matched to the equivalent rate used in a conventional full spectrum sweep to prevent artificial broadening. For example, if a 100 G sweep is conventionally acquired in 60 s without broadening, a 20 G segment must be acquired at a rate no faster than 12 s to maintain a constant rate of passage through the resonance.

Here the nomenclature of the Welch FFT procedure for power spectral density is adopted, due to the similarity of segmentation of a discretized signal, with variables illustrated in

Fig. \ref{fig:Variables}. \citep{WelchFFT} The data are processed in the following manner, as illustrated in Fig. \ref{fig:overlap_add_filt}:

\begin{enumerate}

\item Data are collected at a series of field steps $\delta\phi$ in mT.

\item The data are discretized and windowed to the appropriate length $L\phi$. The length $L\phi$ is determined by the number of points in a discretized field step $n\phi$ (shift step size) multiplied by the overlap factor ϕ_m . The discretized shift step size $n\phi$ can be estimated by

$$n \approx \left\lfloor \frac{N}{\phi_m} \right\rfloor$$

where N is the number of points in the sweep (e.g. 4096), $\phi\phi$ is the field sweep length in mT, and $\phi\phi$ is the field step in mT. The length of the window $L\phi$ and the number of points in a sweep N can be equal, but the windowing can be independent of the total number of points if edge effects (i.e. rapid scan turning points) need to be eliminated. The ratio of the field sweep length and step size yields a maximum overlap value ϕ_m . The shift step size $n\phi$ is rounded to the nearest integer. The integer ϕ_m is a multiplier of $n\phi$ used for segmental overlap, generating $x_{k[j]}$, where x_k is a dataset with point $j=0,1,2,\dots,L-1$ and k is the index of total number of segments K . The number of segments are calculated by

$$K = \left\lfloor \frac{t}{s} \right\rfloor$$

where t is the total spectral sweep width in mT. The ratio is chosen such that K is an integer. No overlap exists at $\phi_m=1$ and symmetric overlap requires ϕ_m as an odd number.

\item The data are zero filled with ϕ_D points to the total discretized length of $\tilde{x}[i]$ with ϕ_D being step shifted by $n\phi$ to align the segments by absolute field.

\item The data are Fourier transformed (FFT) and, in this work, a fixed width Gaussian filter is applied, defined by

$$\text{H}_k(\omega) = \exp\left(-\frac{(\omega - \gamma)^2}{2\sigma^2}\right)$$

where ω is the discretized frequency, γ in the central point in the Fourier transformed data and has a variance of σ^2 . The smallest variance σ^2 which shows no spectral broadening is chosen for each $L\phi$.

\item Filtered data are concatenated to yield $G_{\text{tot}}(\omega)$ which is Inverse Fourier transformed (IFFT) resulting in a filtered whole spectrum $y_{\text{tot}}[i]$. The spectrum is truncated to remove the head and tail (data without overlap) by removing the first and last $L\phi$ points and $y_{\text{tot}}[i]$ is decimated to a conventional number of points, such as 4096.

\end{enumerate}

Signal to noise is calculated by the ratio of the acquired signal mean to the standard deviation of the noise voltage, defined by

\subsection{Continuous-Wave EPR}

Three concentrations of $\text{[FeFe]-hydrogenase}$ from *Chlamydomonas reinhardtii* (single reduced $[\text{Fe-4S}]^{\text{S=1/2}}$, $S=1/2$) were prepared at 1-mM, 100- μM , and 10- μM and confirmed by UV-VIS absorption at 400-nm \citep{Knorzer06012012}. All spectra were collected at 15-K with an incident microwave power of 0.63-mW and a field modulation amplitude of 0.5-mT at 100-kHz. The 1-mM reference spectrum was collected as a single 4-min scan over 100-mT with 4096 points. The 100- μM and 10- μM concentrations were each collected with 25 averages (4-min scan, 100-mT, 4096 points) for a total measurement time of 100-min.

For the SOFFA-CW experiments, the center field was stepped in 0.5-mT increments over a total sweep of 100-mT, yielding $K=200$ steps, with a segment sweep width $\phi_g=25$ -mT and 4096 points per segment. Each segment was collected over 30-s for a total measurement time of 100-min. Segments were acquired using a ProDEL script in Bruker Xepr (v.2.6b-160), which steps the center field and stores each segment in Bruker DSC/DTA format. \footnote{The ProDEL script and Python GUI used to collect and process SOFFA data are available at <https://github.com/jsidabras/SOFFABruker>. \label{foot:github}} The ProDEL script iterates discrete

static field steps, triggers acquisition at each position, and saves the resulting 2D dataset. Software overhead is negligible; the acquisition rate is limited by the hardware field-settling time of the magnet between steps. This approach has been validated for field sweeps up to 8192 points with 1200 steps (0.01-mT step size over 12-mT).

These CW EPR spectra were collected on a Bruker E500 Elecsys X-band spectrometer (9.70-GHz) equipped with a bismuth germanate (Bi₂(GeO₄)₃, BGO) dielectric resonator retrofitted in a Bruker MD5 housing.~\citep{IVANOV201683}

\subsection{Non-Adiabatic Rapid Scan}

The conventional CW comparison and NARS spectra were collected on a custom-built X-band bridge dedicated to segmented-NARS spectroscopy~\citep{HydeSidabrasStrangeway}. A 150- μ m site-directed spin-labeled Hemoglobin sample in 82% glycerol was measured at 18 π in a five-loop--four-gap loop-gap resonator at 9.81-GHz. For the conventional CW reference, 16 averages of 2-min scans were collected over 20-mT with 0.1-mT field modulation at 100-kHz, a 5-ms time constant, and 1-mW of incident microwave power. For the SOFFA-NARS experiment, the static field was stepped in 0.025-mT increments with an overlap of $\Delta=40$, using a trapezoidal field ramp at 11.33-kHz with a 50- μ s flat region and an amplitude of 0.5-mT. Data were acquired over 95% of the trapezoidal sweep in one direction; the resulting edge effects appear as periodic noise outside the signal power spectral density and are suppressed by segment-overlap averaging. Both experiments required approximately 32-min of measurement time.

\subsection{Signal-to-noise Definition}

Signal-to-noise ratio is defined as

$$\text{SNR} = \frac{S_{\text{pk}}}{2\sigma_{\text{noise}}}$$

where S_{pk} is the mean value of the peak to peak (or peak for absorption spectra) signal, and σ_{noise} is the standard deviation of the noise.~\citep{schroeder2000astronomical, oppenheim1999discrete} The standard deviation of the noise is calculated in Mathematica using points in an off-resonance region.

\subsection{Filtering Tests of Simulated Data}

Simulated data of a Gaussian was used to represent an absorption spectrum. Two simulations were performed to test the SOFFA algorithm. The first simulation used strictly random (white) noise and was generated in Mathematica using the `RandReal` function with a `[max]` and `[min]` range defined in such a way that the signal to noise ratio was approximately 4 for a single unfiltered scan. The `RandReal` function is a uniformly distributed pseudo-random number generator, see Fig.~\ref{fig:ShapeNoise}(v). The second simulation used frequency dependent (pink) noise created in Mathematica using the `AudioGenerator["Pink"]` function to generate pseudo-random-frequency dependent noise. This noise was added to a white noise which established a noise floor, see Fig.~\ref{fig:ShapeNoise}(v), such that the signal to noise of a single unfiltered scan was 10. Pink noise was then added to decrease the signal to noise to approximately 4 for a single unfiltered scan.

Each data point in the simulation was repeated 100 times to obtain statistically converged results. For simulated spectra, the 95% confidence interval is shown as an indication of the precision of the estimated mean. Each point was tabulated and plotted alongside conventional averaging for comparison. Segmented data was generated by stepping a window across a noiseless spectrum and generating noise at each step. Each step had an $n=20$ and 6000 points. A total of 500 steps were generated over the spectrum. The overlap Δ was varied and each point was either filtered after concatenation and decimation (Post Add Filter; Methods of Ref.~\citep{HYDE201315}) or filtered in Fourier space and concatenated (SOFFA). For the continuous wave simulation the unfiltered (Raw) data had 4096 points and a low effective time constant. The data was then filtered using the same Fourier transform Gaussian filter. This was repeated for both white and pink noise. The filter variance σ_n^2 was chosen as small as possible without showing spectral broadening. For conventional averaging, the spectral bandwidth of the signal remained constant and a standard deviation of $\sigma_n=35$ was used. Similarly, the spectral bandwidth for filtering after decimation (Post Add Filter) is constant and a standard deviation of $\sigma_n=30$ was used. For the SOFFA method, the spectral bandwidth is a function of Δ and, therefore, must be found for each overlap. Values are tabulated in Table~\ref{table:chars}.

\section{Theory}

In this work, linear noise is assumed, such that,

where S_{pk} is the peak-to-peak signal amplitude and σ_{noise} is the standard deviation of the noise, computed from an off-resonance region of the spectrum.~\citep{schroeder2000astronomical, oppenheim1999discrete}

\section{Theory and Implementation}

The SOFFA data acquisition method consists of four distinct processing stages: (i) oversampling spectral segments, (ii) Fourier block-filtering, (iii) segment-overlap averaging, and (iv) decimation. The nomenclature of the Welch FFT procedure for power spectral density estimation~\citep{WelchFFT} is adopted throughout, due to the similarity of spectral segmentation to that procedure. Table~\ref{table:variables} defines all symbols used in this work, with a graphic representation in Fig.~\ref{fig:Variables}.

\begin{figure}[htbp]

\begin{center}

\includegraphics{S2-Variables.eps}

\caption{Illustration of spectral segmentation with parameters and variables.}

\label{fig:Variables}

\end{center}

\end{figure}

\begin{table*}[htb]

```

\caption{Variables and symbols used in this work.}
\label{table:variables}
\begin{tabular}{l}
\topline
Symbol & Definition & Units/Notes \\
\middleline
\multicolumn{3}{l}{\textit{(i) Acquisition and Sweep Parameters}} \\
\textit{t} & Total spectral sweep width & mT \\
\textit{N} & Number of points per conventional spectrum & -- \\
\textit{s} & Field step size & mT \\
\textit{K} & Total number of segments ( $K = t/s$ ) & -- \\
\textit{t}_e & Total experiment time & s \\
\textit{\tau} & Scan time per segment & s \\
\textit{m}_a & Number of conventional averages & -- \\
\middleline
\multicolumn{3}{l}{\textit{(ii) Segmentation Parameters}} \\
\textit{g} & Segment sweep width & mT \\
\textit{m} & Overlap factor ( $m = g/s$ ) & -- \\
\textit{n} & Discretized shift-step size ( $n \approx N/(g/s)$ , rounded to nearest integer) & points \\
\textit{L} & Segment window length & points \\
\textit{k} & Segment index ( $k = 0, 1, \dots, K-1$ ) & -- \\
 $x_{k[j]}$  &  $k$ -th acquired segment,  $j = 0, 1, \dots, L-1$  & -- \\
 $\tilde{x}_{[i]}$  & Zero-filled, field-aligned segment & -- \\
\textit{D} & Zero-fill offset, shift-stepped by  $n$  to align field positions & points \\
\middleline
\multicolumn{3}{l}{\textit{(iii) Filter Parameters}} \\
 $\omega$  & Discretized frequency index & -- \\
 $\gamma$  & Center point in Fourier domain & -- \\
 $\sigma_n^2$  & Gaussian filter variance & -- \\
 $H_k[\omega]$  & Gaussian filter kernel for segment  $k$  (Eq.~\ref{eq:filter}) & -- \\
 $Y_k[\omega]$  & Fourier transform of segment  $\tilde{x}_{k[i]}$  & -- \\
 $G_k[\omega]$  & Filtered Fourier segment ( $Y_k[\omega] \cdot H_k[\omega]$ ) & -- \\
 $G_{\text{tot}}[\omega]$  & Sum of all filtered segments in Fourier space & -- \\
 $Y_{\text{tot}}[1]$  & IFFT of  $G_{\text{tot}}[\omega]$ , final filtered spectrum & -- \\
\middleline
\multicolumn{3}{l}{\textit{(iv) Noise and SNR Quantities}} \\
 $S(t)$  & True signal & -- \\
 $N(t)$  & Noise (spectrally flat (white) or 1/f (pink)) & -- \\
 $S_{\text{pk}}$  & Peak-to-peak signal amplitude & -- \\
 $\sigma_{\text{noise}}$  & Standard deviation of noise (off-resonance region) & -- \\
OSR & Oversampling ratio ( $= f_s / (2 f_{\text{cw}})$ ) & -- \\
 $f_s$  & Effective sampling frequency ( $= 1/\tau_c$ ) & Hz \\
 $f_{\text{cw}}$  & Spectral bandwidth of conventional CW experiment & Hz \\
 $\tau_c$  & Effective time constant ( $= t_e / (nK)$ ) & s \\
 $\tau_{\text{cw}}$  & Conventional CW time constant & s \\
\bottomline
\end{tabular}

```

Here, linear noise is assumed, such that,

$$\tilde{x}(t) = S(t) + N(t),$$

where $S(t)$ is the signal that is detected and $N(t)$ is either random (white) or frequency dependent (pink) noise. Noise that is a function of the signal is beyond the scope of this work.

For conventionally acquired data, the number of points, scan rate, and time constant are chosen to represent the spectrum completely and without spectral distortions, simulated data for visualization are shown in Fig.~\ref{fig:test data}A. For each new scan, the noise is uncorrelated, therefore, the data can be averaged and filtered. For example, filtered data of Fig.~\ref{fig:test data}A are shown in Fig.~\ref{fig:test data}C. Fourier filtering averaged data before or after summing the individual scans is equivalent. With traditional averaging, the signal to noise follows a strict $\sqrt{m_a}$ gain, where m_a is the number of averages. The same signal/time trade off exists when increasing the number of collected data points while maintaining equivalent measurement time.

If a signal input is infinitely long or for signals that need to be filtered in real time, the Overlap Add method is used with short time Fourier transform (STFT) block filtering for efficient digital signal processing. \citep{oppenheim1999discrete, ifeachor2002digital} Block filtering breaks a long or continuous signal $x(t)$ into a series of spectral windows with a fixed discrete length. Each window is filtered individually in Fourier space and concatenated back together, as illustrated in Fig.~\ref{fig:schemes}A. Finite impulse response (FIR) filters with block filtering are easily implemented and will be the focus of this work. Finally, the output of block filtering and recombining the data with an Overlap add or Overlap save method is equivalent to filtering the long signal $x(t)$ data directly.

\begin{figure}[htb]
\begin{center}

```

\includegraphics[width=0.4\textwidth]{02_scheme.eps}
\caption{(A) The Overlap Add filter design is used for a large time domain signal  $x(t)$  where it is discretized  $\tilde{x}[l]$  and segmented by delayed blocks  $\Delta$ . Each discretized window is Fourier filtered by  $\omega$  and concatenated. (B) In a segmented magnetic resonance experiment, each overlapped segment has noise that is uncorrelated. Each segment is discretized separately, Fourier filtered by  $\omega$ , and overlapping segments are further averaged during concatenation. Without overlap ( $L=1$ ) the methods of (A) and (B) are equivalent.}
\label{fig:schemes}
\end{center}
\end{figure}
\begin{figure}[htb]
\begin{center}
\includegraphics{03_TestData.eps}
\caption[A Gaussian absorption spectrum is simulated with a half width of 1 mT and an amplitude of unity. Shown here is a representation of the simulated experiment. (A) Random (white) noise is added. (B) Small set of unfiltered segmented data are plotted showing field steps  $\delta$ . Illustration of segmentation is shown in the inset. (C) When a Gaussian convolution filter of Eq. \ref{eq:filter} is applied to (A), the expected improvement in signal to noise is shown, similar to increasing the time constant. (D) However, as  $L$  is increased, further signal to noise improvement is exhibited due to the concatenation of filtered data per the SOFFA method. This experiment is repeated 100 times and the mean of the signal to noise ratios are plotted for white and pink noise, Figs. \ref{fig:FiltChars}A and \ref{fig:FiltChars}B, respectively. white and pink noise data are tabulated in Table \ref{table:chars}.]
\label{fig:test-data}
\end{center}
\end{figure}
In this section the four processes utilized to create the SOFFA data acquisition method are detailed: (i) Oversampling Spectral Segments, (ii) Fourier Block Filtering each segment separately, (iii) Segment overlap averaging, and (iv) Decimation. It is the combination of these processes that improves the signal to noise ratio for the same amount of data collection time.
\subsection{Oversampling Spectral Segments}
When implementing a block filter approach, the discretized continuous input signal must be down sampled by the number of blocks and then, after filtering, up sampled and concatenated. \citep{oppenheim1999discrete} The down and up sampling ratios do not have to be equivalent and each block could have overlapping segments. \citep{OverlapBlock} For example, if an input signal has 4096 points, a series of 32 blocks can be formed without overlap with  $L=128$ . The advantage of employing block filtering is the ability to process the blocks in parallel, illustrated in Fig. \ref{fig:schemes}A, and speed up the convolution process for real time processing or for continuous discrete signals.
When implementing traditional block filtering, segments are generated by windowing the whole signal where the windowing function with window size  $L$ , which yields a long signal segmented into  $k$  segments with the length of  $L$  ( $i=0,1,\dots,L-1$ ) separated by  $n$ , which is the discretized window step delay size. Once windowed and Fourier transformed, each discretized signal is considered a Short time Fourier transform (STFT) and can be filtered in Fourier space with convolution techniques. Since each segment is generated from a single input the noise is correlated and an appropriate windowing function  $w[i,n]$  is required to minimize processing noise and aliasing artifacts. \citep{FFTWindowing} When each block is recombined using the Overlap add or Overlap save algorithm, the signal to noise of the filtered signal is exactly equivalent as if the whole signal was processed directly.
where  $S(t)$  is the signal that is detected and  $N(t)$  is either spectrally flat (white) noise, characterized by a frequency-independent power spectral density, or  $1/f$  (pink) noise, characterized by a power spectral density that increases with decreasing frequency. Noise that is a function of the signal is beyond the scope of this work.
For conventionally acquired data, the number of points, scan rate, and time constant are chosen to represent the spectrum completely and without spectral distortions, simulated data for visualization is shown in Fig. \ref{fig:test-data}A. For each new scan, the noise is uncorrelated, therefore, the data can be averaged and filtered. For example, filtered data of Fig. \ref{fig:test-data}A is shown in Fig. \ref{fig:test-data}C. Fourier filtering averaged data before or after summing the individual scans is equivalent. With traditional averaging and white noise, the signal-to-noise follows a strict  $\sqrt{m_a}$  gain, where  $m_a$  is the number of averages. The same signal/time trade-off exists when increasing the number of collected data points while maintaining equivalent measurement time.
In the following sections, the four processes utilized to create the SOFFA data acquisition method are detailed: (i) Oversampling Spectral Segments, (ii) Fourier Block-Filtering each segment separately, (iii) Segment-overlap averaging, and (iv) Decimation. It is the combination of these processes that improves the signal-to-noise ratio for the same amount of data collection time.
\subsection{Oversampling Spectral Segments}\label{sec:oversampling}
In the SOFFA data acquisition method, each field/frequency swept segment has the following properties: (i) the overlapping noise is non-coherent, (ii) field- or frequency-dependent features are considered signal, and (iii) each segment is an oversampled section of the whole spectrum. In the case of the SOFFA method, all segments are collected separately and can then be further windowed to the desired length to remove potential edge effects the windowing function with window size  $L$ . Stepping  $s$  over the spectrum yields  $k$  individually collected segments. Each segment is offset by the discrete shift-step size  $n$ . Since magnetic resonance produces a stationary and time-invariant signal, the corresponding output blocks can be zero filled by a length of the total collection size to begin at the same absolute step size, aligning the field or frequency dependent features. The zero-fill parameter is then shift-stepped by  $n$  to align field dependent features. To maximize the overlap averaging after filtering, the windowing function is chosen to be

```

rectangular and no aliasing issues exist if oversampling is used. Unlike windowing in typical block-filtering, which benefits greatly from window choice \citep{FFTWwindowing}, a rectangular window will maximize the individual contribution of each segment during the concatenation process. Any higher order frequencies generated by discontinuities are removed in the filtering process and result in proper concatenation and aliasing.

@@ -246,28 +264,48 @@

where f_{cw} is the inverse of the time constant τ_{cw} of the conventional CW data collection.

~~Signal to noise is improved in oversampling by reducing the spectral bandwidth by the OSR and effectively spreading noise power spectral density by the same amount, see Fig. \ref{fig:ShapeNoise} (\textit{ii} and \textit{iii}). \citep{oppenheim1999discrete} Since segmented magnetic resonance spectra are collected, a further decrease the spectral bandwidth is exhibited since only a fragment of the spectrum is sampled.~~

~~Once each of the segments is sufficiently oversampled, noise shaping can be employed to reduce the high-frequency content outside the spectral bandwidth by applying finite impulse response (FIR) block-filtering techniques.~~

Signal-to-noise is improved in oversampling by reducing the spectral bandwidth by the OSR and effectively spreading noise power spectral density by the same amount, see Fig. \ref{fig:ShapeNoise} (\textit{ii} and \textit{iii}). \citep{oppenheim1999discrete} Since segmented magnetic resonance spectra are collected, a further decrease in the spectral bandwidth is exhibited since only a fragment of the spectrum is sampled. Ultimately, the bandwidth of the noise increases but it is the reduction of the bandwidth of the signal (due to the collection of partial spectra) that is reduced, resulting in a more aggressive filter without spectral broadening.

A key advantage of the segmented acquisition strategy is that it allows the whole spectrum to be oversampled far beyond what the spectrometer hardware permits in a single continuous sweep. Legacy instruments such as some Bruker E500 consoles are limited to 8192 points per continuous sweep. With SOFFA, collecting a spectrum with a 2-mT segment sweep width, a 0.1-mT field step size, 4096 points per segment, and 100 steps produces 204,800 effective data points across the whole spectrum. Because the magnetic resonance signal is stationary and time-invariant, the signal contribution from every segment that covers a given field position is fully correlated, meaning the same EPR line appears at the same field value in each overlapping segment. The noise, however, is generated independently at each acquisition and is therefore uncorrelated between segments. The result is a whole-spectrum dataset with correlated signal and uncorrelated noise, which is precisely the condition that enables effective Fourier filtering and signal averaging to improve the signal-to-noise ratio. Another advantage of oversampled segmented data collection has to do with noise that is loosely correlated to the signal or noise that is colored, such as $1/f$ noise. In conventional CW, the time constant acts as a low-pass filter on the data, while the sweep duration acts as a high-pass filter on the noise. When one sweeps through a whole spectrum and repeats for averaging, one averages in $1/f$ noise which has a power spectral density that cannot be directly filtered without broadening the EPR signal and any correlated noise is averaged in reducing the effectiveness of averaging (yields \sqrt{m}). However, by reducing the sweep into segments and maintaining the sweep rate (e.g. 60 seconds for 10-mT compared and 12 seconds for 2-mT) the shorter observation window inherently rejects ultra-low-frequency drift. Furthermore, due to the segment step timing and excessive overlap, any remaining correlated noise is randomized between segments. This decorrelation allows the signal averaging to approach the theoretical white-noise limit of \sqrt{m} . Once each of the segments is sufficiently oversampled, filtering can be employed to reduce the high frequency content outside the spectral bandwidth by applying finite-impulse response (FIR) block-filtering techniques.

\subsection{Fourier Block-Filtering each Segment Separately}

~~The SOFFA data acquisition method differs from typical Fourier Block-Filtering by two important factors: (i) Each segment is a new collection of data with field- or frequency-stepped correlated signal and uncorrelated noise and (ii) each segment overlaps the next segments for a total of m overlapping segments. Due to oversampling, the spectral bandwidth of the spectrum in each segment is reduced, see Fig. \ref{fig:ShapeNoise} comparing spectra \textit{ii} and \textit{iii}.~~

~~Fourier block-filtering is illustrated in Fig. \ref{fig:schemes}. Each segment is convolved with the filter $H(\omega)$, such that~~

The SOFFA data acquisition method differs from typical Fourier Block-Filtering by two important factors: (i) Each segment is a new collection of data with field- or frequency-stepped correlated signal and uncorrelated noise and (ii) each segment overlaps the next segments for a total of m overlapping segments, Fig. \ref{fig:test-data}. Due to oversampling, the spectral bandwidth of the spectrum in each segment is reduced, see Fig. \ref{fig:ShapeNoise} comparing spectra \textit{ii} and \textit{iii}.

Fourier block-filtering is illustrated in Fig. \ref{fig:schemes}. Each segment is convolved with the filter $H(\omega)$, such that

$$\begin{equation} \text{G}_k(\omega) = \text{Y}_k(\omega) \text{H}_k(\omega), \end{equation}$$

~~where $\text{Y}_k(\omega)$ is the Fourier transform (Fourier space ω) of the discrete signal and the convolution is $\text{G}_k(\omega)$. In this work, a fixed FIR Gaussian filter is used, see Eq. \ref{eq:filter}. However, it should be noted that these filters do not have to be fixed and can vary at each k value, or be more sophisticated, such as adaptive averaging techniques. \cite{COCHRANE200817,Manning2020}~~

~~Spectral leakage occurs when the chosen Gaussian standard deviation σ_n is more narrow than the spectral bandwidth of the desired signal. As the length of L is increased for each segment, the OSR must be increased to maintain the same spectral bandwidth. However, in practice this is~~

~~impractical and, instead, the standard deviation of the filter must be modified to ensure no spectral leakage. By choosing to adjust σ_n , the spectral bandwidth will approach that of the whole spectrum as L approaches the total length of $\tilde{x}[i]$ ($i=0,1, \dots, N$) and the signal-to-noise improvement will approach that of filtering after concatenation (Post-Add Filter) as employed by Hyde [et al.](#) [\[HYDE201315\]](#)~~

~~Since the optimum windowing method for the SOFFA algorithm is rectangular, abrupt discontinuities may exist in field space as the data are collected segmentally. Discontinuities cause Sinc-like features in Fourier space. However, Fourier filtering each segment with an FIR Gaussian filter removes these discontinuities and produces smooth overlap and concatenation. Filtering each segment separately removes the need for filtering the periodic noise associated with the step as in~~

where $Y_k[\omega]$ is the Fourier transform (Fourier space ω) of the discrete signal and the convolution is $G_k[\omega]$. In this work, a fixed FIR Gaussian filter is used, defined by

$$H_k[\omega] = \exp\left\{-\frac{(\omega - \gamma)^2}{2 \sigma_n^2}\right\},$$

where ω is the discretized frequency, γ in the central point in the Fourier transformed data and has a variance of σ_n^2 . The smallest variance σ_n^2 which shows no spectral broadening is chosen for each L . However, it should be noted that these filters do not have to be fixed and can vary at each k value, or be more sophisticated, such as adaptive averaging techniques.

[\[COCHRANE200817, Manning2020\]](#)

Spectral leakage occurs when the chosen Gaussian standard deviation σ_n is more narrow than the spectral bandwidth of the desired signal. As the length of L is increased for each segment, the OSR must be increased to maintain the same spectral bandwidth. However, in practice this is impractical and, instead, the standard deviation of the filter must be modified to ensure no spectral leakage. By choosing to adjust σ_n , the spectral bandwidth will approach that of the whole spectrum as L approaches the total length of $\tilde{x}[i]$ ($i=0,1, \dots, N$) and the signal-to-noise improvement will approach that of filtering after concatenation (Post-Add Filter) as employed by Hyde [et al.](#) [\[HYDE201315\]](#)

Since the optimum windowing method for the SOFFA algorithm is rectangular, abrupt discontinuities may exist in field space as the data is collected segmentally. Discontinuities cause Sinc-like features in Fourier space. However, Fourier filtering each segment with an FIR Gaussian filter removes these discontinuities and produces smooth overlap and concatenation. Filtering each segment separately removes the need for filtering the periodic noise associated with the step as in

[Ref.](#) [\[HYDE201315\]](#), which is required if the spectrum is filtered after concatenation as in Post-Add Filter.

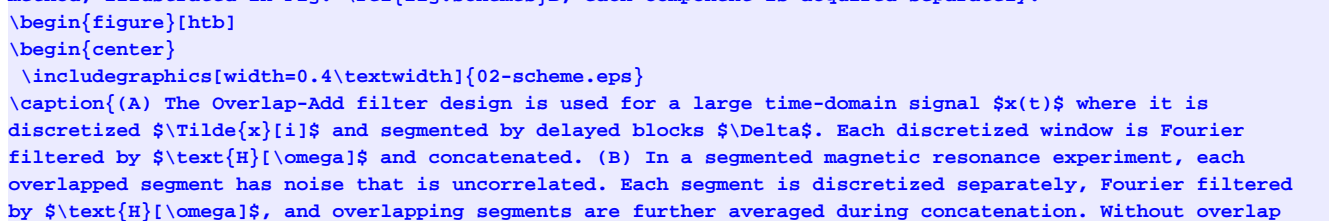
As m increases the length of the tail further overlaps with the head of multiple segments resulting in averaging.

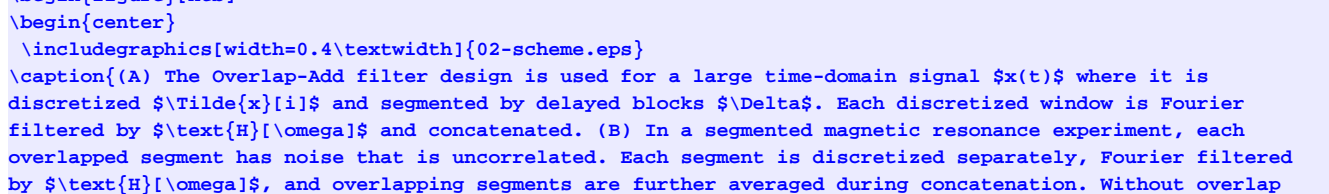
~~The SOFFA methodology is equally applicable to spectra containing well resolved, narrow hyperfine features, provided that acquisition and processing parameters are scaled accordingly. To maintain spectral integrity and prevent artificial broadening, the variance of the Gaussian filter (σ_n^2) in the Fourier block filtering stage must be minimized relative to the intrinsic linewidth. Additionally, the field step size (δ) serves as a high precision parameter to control the effective oversampling ratio (OSR) and the resulting number of overlapped segments. While decreasing δ allows for fine tuning the signal to noise ratio (S/N) via increased overlap density, it is ultimately constrained by hardware performance. On spectrometers such as the Bruker E500, the practical limit for δ is approximately 0.1 G, with 0.25 G representing a conservative threshold to ensure field controller precision and mitigate the effects of magnet hysteresis. For large scale multiplicative improvements in S/N, it is recommended to increase the number of full stack repetitions, whereas adjusting the step size δ should be reserved for fine scale optimization of the overlap density.~~

Segment-Overlap Averaging

~~Once each segment is successfully filtered, the segments must be concatenated together. Due to the use of a rectangular window, the segments can be concatenated in Fourier space, to save processing time, and a single inverse Fourier transform (IFFT) is needed to obtain the discretized spectrum. Because the data are zero filled and aligned, this is done simply by summation~~

If a signal input is infinitely long or for signals that need to be filtered in real time, the Overlap-Add method is used with short-time Fourier transform (STFT) block-filtering for efficient digital signal processing. [\[oppenheim1999discrete, ifeachor2002digital\]](#) Block-filtering breaks a long or continuous signal $x(t)$ into a series of spectral windows with a fixed discrete length. Each window is filtered individually in Fourier space and concatenated back together, as illustrated in [Fig. A](#). Finite-impulse response (FIR) filters with block-filtering are easily implemented and will be the focus of this work. Finally, the output of block-filtering and recombining the data with an Overlap-add or Overlap-save method is equivalent to filtering the long signal $x(t)$ data directly. In the case of the SOFFA method, illustrated in [Fig. B](#), each component is acquired separately.





(A) The Overlap-Add filter design is used for a large time-domain signal $x(t)$ where it is discretized $\tilde{x}[i]$ and segmented by delayed blocks Δ . Each discretized window is Fourier filtered by $H[\omega]$ and concatenated. (B) In a segmented magnetic resonance experiment, each overlapped segment has noise that is uncorrelated. Each segment is discretized separately, Fourier filtered by $H[\omega]$, and overlapping segments are further averaged during concatenation. Without overlap

(\$L=1n\$) the methods of {\bf A} and {\bf B} are equivalent.}

```
\label{fig:schemes}
\end{center}
\end{figure}
```

When implementing traditional block-filtering, segments are generated by windowing the whole signal where the windowing function with window size \$L\$, a long signal segmented into \$K\$ segments with the length of \$L\$ (\$i=0,1,\dots,L-1\$) separated by \$n\$, which is the discretized window step delay size. Once windowed and Fourier transformed, each discretized signal is considered a Short-time Fourier transform (STFT) and can be filtered in Fourier space with convolution techniques. Since each segment is generated from a single input the noise is correlated and an appropriate windowing function \$w[i-n]\$ is required to minimize processing noise and aliasing artifacts.~\citep{FFTWindowing} When each block is recombined using the Overlap-add or Overlap-save algorithm, the signal-to-noise of the filtered signal is exactly equivalent as if the whole signal was processed directly.

Once each segment is successfully filtered, the segments must be concatenated together. Due to the use of a rectangular window, the segments can be concatenated in Fourier space, to save processing time, and a single inverse Fourier transform (IFFT) is needed to obtain the discretized spectrum. Because the data is zero filled and aligned, this is done simply by summation

```
\begin{equation}
\text{G}_{\text{tot}}[\omega] = \sum_{k=0}^{K-1} \text{Y}_k[\omega] \text{H}_k[\omega].
\end{equation}
```

@@ -278,132 +316,31 @@

```
\subsection{Decimation}
```

~~The total number of points in the final concatenated spectrum \$y_{\text{tot}}[i]\$ is a function of the oversampling rate, the step size, and the number of steps. In order to generate a SOPFA acquired spectrum with a conventional number of points, decimation is used. Decimation acts as a moving average while reducing the total number of points. Herein a nearest neighbor windowing approach is used where \$M\$ number of points are averaged together and replaced by one new point, where \$M\$ is the re-sampling ratio. The decimation process is designed to conserve the cumulative improvements generated by the upstream SOPFA processes while reducing the data to a standard spectral representation. This stage acts as a final digital low pass filter on the system, providing an additional enhancement proportional to the square root of the decimation factor (\$\sqrt{M}\$). For example, decimating a segment from 8192 points to 2048 points (\$M=4\$) yields a potential improvement factor of 2. By effectively narrowing the noise bandwidth to the final spectral resolution, decimation ensures that the benefits of high rate oversampling are fully realized in the final output.~~

```
\subsection{Summary}
```

~~The aforementioned processes provide a framework for the SOPFA data acquisition method. It should be noted that if the filter \$H[\omega]\$ is constant, as defined in this work, the output \$y[i]\$ will be equivalent if block filtering is used or the oversampled data are filtered after concatenation, but before decimation. By filtering after decimation (Post Add Filter), the filtering effectiveness is reduced compared to the SOPFA method. If the filter varies for each segment \$H_k[\omega]\$ it is no longer possible to obtain an equivalent filtering after concatenation, but before decimation. \citep{OverlapBlock,KARAMI2018209} Thus, the block filtering approach employed by the SOPFA method provides more flexibility in filter design. Effectively, the SOPFA data acquisition method splits data processing into two categories: (i) high frequency filtering and noise shaping and (ii) low frequency averaging.~~

~~Furthermore, the SOPFA data acquisition method effectively circumvents the hardware based memory limitations inherent to older spectrometers. Legacy systems, such as certain Druker E500 consoles, are often restricted to a maximum of 4096 data points per continuous sweep. By segmenting the acquisition, SOPFA decouples the total experimental resolution from these hardware constraints. For example, acquiring a 100-G spectrum using 1-G steps and 20-G segments, where each segment utilizes 4096 points, results in an effective acquisition of 204,800 data points across the full spectral width. This yields a massive effective oversampling ratio that is impossible to achieve in a single conventional sweep on legacy hardware.~~

```
\section{Results and Discussion}
```

```
\subsection{Simulated Gaussian Absorption Spectrum}
```

```
\begin{figure}[!htb]
```

```
\begin{center}
```

```
\includegraphics{04_FilteringChars.eps}
```

~~\caption{Signal to noise mean and 95\% confidence interval (CI) of 100 simulations of a simulated Gaussian absorption spectrum with additive (A) white Noise and (B) pink Noise. Post Add filter, with a fixed variance \$\sigma_n=30\$ is shown as \$\circ\$, while the SOPFA data acquisition method with the a variable variance \$\sigma_n\$ is plotted as \$\blacklozenge\$. Dotted lines are the expected \$\sqrt{m}\$ from averaging starting at SOPFA with no overlap \$m\$ is one/ 71.5. Dashed lines are the traditional averaging, which follows a strict \$\sqrt{m-a}\$ starting at a single scan \$m-a\$ is one/ 33.0. Data are normalized to the mean of the \$m_a=1\$ value of the traditional averaging with white and pink noise, respectively. Data are tabulated in Table \ref{table:chars}. Simulated spectral parameters are identical to those described in Fig. \ref{fig:test data}.~~

```
\label{fig:FiltChars}
```

```
\end{center}
```

```
\end{figure}
```

~~Segmented data are simulated with Fourier filtering (\$\sigma_n=30\$) performed after decimation (Post Add Filter; \$\circ\$), and an increase in signal to noise is shown related to the length of the overlap \$m\$, shown in Fig. \ref{fig:FiltChars}. The Post Add Filter is similar to the segmented NARS methodology which has been previously reported and analyzed. \citep{HYDE201315} In this study, Post Add Filtered data does not perform better than traditional averaging. However, this simulated study only characterizes the~~

signal to noise assuming all experiments take the same amount of time. Further practical improvements are expected when accounting for the step size, oversampling rate, scan time, and conventional averaging time. For example, it is possible to create experimental parameters where 50 steps have an overlap of $\sigma=200$ and take the same total measurement time of conventional averaging of 50 total averages. Finally, segmented data are simulated and processed with the SOPFA method. When $\sigma=1$, no overlap is present and the SOPFA method produces a factor of 2.2 (71.5:33.0) compared to filtering the conventional averaging (Trad. Ave.) spectra for white noise and a gain of 1.7 (15.2:9.1) for pink noise. As the number of overlap segments increases the gain at $\sigma=200$ exhibits a factor of 2.4 (1101:467.3) for white noise or a potential of 1.4 (213.0:157.7) is realized when pink noise dominates. The improvement shown between the SOPFA $\sigma=1$ data and conventional averaging $\sigma_a=1$ is due to filtering oversampled segments and decimation of the concatenated whole spectrum. Data are tabulated in Table [\ref{table:chars}](#).

	Trad. Ave.)			Post Add Filter			SOPFA				
σ	σ_n	SNR _W	SNR _P	σ	σ_n	SNR _W	SNR _P	σ	σ_n	SNR _W	SNR _P
1	35.0	33.0	9.1	30.0	32.9	14.78	25.0	71.5	15.2		
5	73.9	21.2	5	80.2	10.1	20.0	192.6	22.1			
10	104.5	29.1	10	100.4	22.5	17.5	292.4	27.2			
20	147.8	39.1	20	155.1	32.0	20.0	386.6	35.5			
30	181.0	49.7	30	194.9	41.1	20.0	520.7	45.8			
50	233.6	64.1	50	246.4	55.9	22.5	625.7	62.6			
100	330.4	92.2	100	349.4	84.7	27.5	963	97.2			
200	467.3	131.1	200	491.8	120.0	45	1101	152.3			
300	573.1	157.7	300	675.2	164.6	70	1092	213.0			

It is clear from Fig. [\ref{fig:FiltChars}](#) that the SOPFA method (σ) performs exceedingly well on white noise compared to both conventional averaging (dashed) and the Post Add Filter methods (σ) of Ref. [\citep{HYDB201315}](#). In Fig. [\ref{fig:FiltChars}A](#), a \sqrt{m} line is plotted normalized to $\sigma=1$ of the SOPFA method (dotted). As the overlap is increased and each dataset uses an optimum σ_n , the improvement compared to \sqrt{m} has a maximum at $\sigma=200$. This suggests there is an optimum overlap and filter combination that is a function of the spectral bandwidth. Additionally, as σ increases the spectral bandwidth approaches that of the whole spectrum. When this occurs, filtering after decimation or with block filtering becomes equivalent if ω is constant.

When dealing with noise dominated by frequency dependent pink noise, the segmented methodology, in general, performs well. Pink noise is considered very difficult to filter since the spectral bandwidth is similar to the EPR spectrum. However, by effectively splitting the high frequency noise floor and averaging the low frequency, the signal to noise can be improved compared to traditional averaging and filtering, shown in Fig. [\ref{fig:FiltChars}B](#). Further improvement reducing pink noise is feasible by including adaptive averaging techniques as the filter ω_k . [\citep{COCHRANE200817, MOVINGADAPT, Manning2020}](#)

Continuous Wave EPR

A series of CW EPR spectra of *apo* [FeFe] hydrogenase from *Chlamydomonas reinhardtii* of varying concentrations were collected using a bismuth germanate (Bi₄(GeO₄)₃, BGO) dielectric resonator retrofitted in a Bruker MD5 housing. [\citep{IVANOV201683}](#) The *apo* protein has one reduced [4Fe 4S]⁺ cluster with an effective S=1/2. Three concentrations of 1 mM, 100 μ M, and 10 μ M were prepared and confirmed with UV-VIS by measuring the characteristic 400 nm feature indicating relative amounts of [4Fe 4S]. [\citep{Knorzec06012012}](#) The conventional CW spectra were collected by a 4 minute scan of 4096 points over 100 mT and averaged 9 times. The 1 mM concentration spectrum, shown in Fig. [\ref{fig:CWapo_Test}A](#) spectrum *i* is intended to be used as a reference. Both the 100 μ M and 10 μ M concentrations were collected with 25 averages for a total time of 100 minutes, shown in Fig. [\ref{fig:CWapo_Test}A](#) spectrum *ii* and *iii*, respectively. Both CW spectra were background subtracted to remove background from the shield. All CW data was filtered with a $\sigma_n=75$. The 100 μ M CW spectrum yielded a signal to noise of 181.8, while the 10 μ M CW spectrum was calculated at 16.5.

A SOPFA CW EPR spectrum was obtained by stepping the field 0.5 mT over 100 mT resulting in 200 steps of 25 mT sweep width (4096 points each). Each segment was collected over 30 seconds for a total time of 100 minutes. A signal to noise improvement of 6.1 (1114:181.8) is exhibited between the 100 μ M CW experiment and the SOPFA CW experiment. The SOPFA CW experiment with 10 μ M concentration was also collected in 0.5 mT steps of 25 mT sweep width over 30 s and 4096 points for a total time of 100 minutes. A total of 200 steps were collected over a 100 mT total sweep. The signal to noise ratio was calculated to be 83.8 and a signal to noise improvement of 5.1 (83.8:16.5) is exhibited for an average of 5.6 increase in concentration sensitivity. All SOPFA CW spectra were block filtered with a $\sigma=50$ and with an $\sigma_a=48$. The EPR feature at 340 mT is a background caused by residual sodium dithionite which is used to reduce the iron sulfur clusters of the *apo* [FeFe] hydrogenase.

[\begin{figure}\[htbp\]](#)
[\begin{center}](#)
[\includegraphics{05_APO_CW.eps}](#)

~~\caption{CW spectra were collected on an Bruker B5180 X band bridge with a dielectric resonator (9.70 GHz) of the reduced [4Fe 4S]⁺ of \textit{apo} [FeFe] hydrogenase from \textit{Chlamydomonas reinhardtii} at 1 mM, 100 μM , and 10 μM concentrations, spectrum \textit{i}, \textit{ii}, and \textit{iii}, respectively. The reference spectrum of 1 mM concentration was collected over 100 mT, 4 minute scans averaged 9 times with 4096 points. The traditional CW experiment with 100 μM concentration was collected over 100 mT, 4 minute scans averaged 25 times with 4096 points for a total time of 100 minutes. Both CW spectra were filtered with a $\sigma_n=75$. The SOFFA CW experiment with 100 μM concentration was collected in 0.5 mT steps of 25 mT over 30 s and 4096 points for a total time of 100 minutes. The SOFFA CW experiment with 10 μM concentration was collected in 0.5 mT steps of 25 mT over 30 s and 4096 points for a total time of 100 minutes. For both SOFFA CW experiments, a total of 200 steps were collected over a 100 mT total sweep. All segments were block filtered with a $\sigma=50$ and with an $\phi_m=40$. All spectra were collected at a temperature of 15 K and at an incident power of 0.63 mW with a field modulation amplitude of 0.5 mT. The spectral feature marked with \ast is a cavity background that overwhelms the 10 μM signal, therefore SNR was taken with the feature at 360 mT.}~~

~~\label{fig:CWApo_Test}~~

~~\end{center}~~

~~\end{figure}~~

~~\subsection{Non adiabatic and Adiabatic Rapid Scan}~~

~~\begin{figure}[htbp]~~

~~\begin{center}~~

~~\includegraphics{06_150uM_Heme.eps}~~

~~\caption{A 150 μM site directed spin labeled Hemoglobin sample in 92\% glycerol at 10 $^{\circ}$ C is collected with conventional CW EPR in a five loop four gap loop gap resonator at X band (9.81 GHz) using 0.1 mT field modulation at a rate of 100 kHz, 5 ms time constant, 16 averages over 20 mT (2 min scan) at 1 mW of microwave power yielding a signal to noise of 9.9. A Gaussian filter was applied to the CW data yielding a signal to noise of 46.9. SOFFA NARS data was collected with 0.25 G steps (ϕ_s) an overlap of $\phi_m=40$ using a trapezoidal field ramp of 11.24 kHz with 6 μs flat rate and an amplitude of 0.5 mT. Processing the data with the SOFFA method results in a signal to noise of the pure absorption signal (not shown) of 3890. An MDIFF pseudo modulation of 0.1 mT field modulation equivalent was used to display the spectrum in a more conventional form, yielding a signal to noise of 483.3. The zoomed inset is the first 500 points of the NARS signal. Data was collected on a custom built X band bridge dedicated to segmented NARS spectroscopy. A NARS dispersion signal was also collected (not shown). Both experiments took approximately 32 minutes each.}~~

~~\label{fig:150uMHeme}~~

~~\end{center}~~

~~\end{figure}~~

~~Conventional CW data was compared to SOFFA NARS of a 150 μM of a site directed spin labeled Hemoglobin sample in 92\% glycerol (10 $^{\circ}$ C) at X band (9.81 GHz), shown in Fig. \ref{fig:150uMHeme}. Experimental parameters are stated in the figure caption. This sample is in the slow tumbling regime of approximately 15×10^9 seconds rotational correlation time τ_{corr} . After 16 averages of 2 min scans a CW signal to noise of 9.9 is realized. Adding a Gaussian filter increases the signal to noise by a factor of 4.7 (46.9/9.9). By processing the segmented NARS data with the SOFFA filtering method, the collected pure absorption signal has a signal to noise of 3890 (data omitted). In order to display the spectrum in a more conventional form, the first derivative is computed using an MDIFF pseudo modulation of 0.1 mT. A signal to noise increase of 10.3 (483.3/46.9 compared to the filtered CW data) was achieved for the same measurement time of 32 minutes. The zoomed inset is the first 500 points of the NARS signal multiplied by a factor of 50. Since NARS uses a balanced mixer and A/D converter, the dispersion signal was also collected for no increase in measurement time (data omitted). The NARS linear background was baseline corrected in Xopr.~~

~~\subsection{Practical Considerations}~~

~~The signal to noise ratio of EPR is fundamental to the usefulness of the technique. Improvements in EPR fall into two categories: technical developments, such as resonator and spectrometer advances, multiharmonic data collection\cite{Yu2015may} and advanced averaging and filtering techniques, such as, wavelet analysis\cite{PreedIEEE} and adaptive averaging\cite{COCHRANE200817, Manning2020} techniques. One must take care that any new method does not over filter and deliver a distorted EPR spectrum.~~

~~In addition, the evaluation of new technology must be done with both random Gaussian noise and correlated 1/f noise under consideration. As describe earlier, Gaussian noise is characterized by the uniform power spectral density in the whole frequency space, plotted in Fig. \ref{fig:ShapeNoise}D(vi). Correlated noise ('Pink' noise), as shown in Figure \ref{fig:ShapeNoise}(v), where a significant portion of the power spectral density is located in low frequencies (1/f) that overlap with the power spectral density of the EPR signal. It is important to note that 'Pink' noise power spectral density is a function of scan time and can be thought of as a measurement of system stability. \cite{KITTELL2011228} Because of this, changing the sweep speed changes the correlated noise of the system.~~

~~In this experiment, the ^{13}C lines of 10 μM TEMPOL have been highlighted by using traditional averaging, shown in black, by scanning 400 times over a 273 minute time period. In contrast, the same signal to noise ratio can be achieved in only 20 minutes (red) without loss of the subtle ^{13}C lines.~~

~~\begin{figure}[!htb]~~

~~\begin{center}~~

~~\includegraphics{08_PhaseNoise.eps}~~

~~\caption{A 10 μM TEMPOL spectrum is recorded using A) traditional CW averaging for 273 minutes (400 averages; black) and using SOFFA CW in 20 minutes (red). On ^{13}C feature is highlighted. The continuous wave experiment was collected with 10 mT sweep of 1024 points over 41.94 seconds with 400 averages, 20.48 ms time constant, at 3.2 mW, 0.1 mT field modulation at 100 kHz. SOFFA CW was performed with 3 mT sweep of 8192 points over 10.39 seconds, with 100 steps of 0.1 mT each, 1.28 ms time constant, at 3.2 mW, 0.1 mT field~~

modulation at 100 kHz. B) Phase noise was averaged for 400 averages and added to the continuous wave data (black) and phase noise was added onto each of the 100 steps of the SOFFA CW (red).]

```
\label{fig:PhaseNoise}
\end{center}
\end{figure}
```

Since the power spectral density of 1/f noise is similar to the EPR signal, both correlated noise and EPR signal have similar shape in the field domain making fitting subtle spectral features difficult without significantly improving the signal to noise ratio of the EPR signal with hardware improvements since excessively long averaging will not average out 1/f noise.

As an example, the EPR spectra of Fig. \ref{fig:PhaseNoise}A was corrupted with 1/f noise by averaging randomly generated correlated noise and adding it to the EPR spectrum. The noise was implemented in the frequency domain following a 1/f power law, establishing a crucial framework for realistic noise modeling in EPR experiments through a systematic process of creating frequency spectra, scaling amplitudes inversely with frequency, and adding random phase components. The implementation maintains mathematical rigor by ensuring conjugate symmetry in the frequency domain, a necessary condition for reconstructing physically meaningful real signals when transforming back to the field domain. The resulting spectrum for continuous wave is shown in black in Fig. \ref{fig:PhaseNoise}B.

For SOFFA, the randomly generated correlated noise was added to each of the 100 segments and averaging was performed through the SOFFA algorithm. Since the continuous wave EPR experiment and the SOFFA CW experiment have different sweep times (41.49 s and 10.39 s, respectively) the frequency content of the correlated noise is different and it taken into account in this experiment. The resulting spectrum for SOFFA CW is shown in red in Fig. \ref{fig:PhaseNoise}B. From this, it is clear that the subtle $\delta^{13}\text{C}$ lines of the 10 μM TEMPOL are lost in the continuous wave EPR spectrum and remain in the SOFFA CW. The SOFFA method demonstrates enhanced EPR spectral features by not only enhancing the signal to noise ratio by a factor of 3.2 compared to traditional continuous wave measurements (1203:367), but also effectively mitigating phase noise and 1/f correlated noise, thereby preserving subtle spectral features such as $\delta^{13}\text{C}$ lines and enabling more reliable spectral fitting even in challenging low concentration samples.

Finally, the version of Bruker Xepr (v.2.6b 160) used to collect the SOFFA spectra is not optimized for segmented data acquisition. Future work will implement segmented NARS using the Xepr Python API interface to decrease the latency associated with large datasets. A signal to noise improvement is expected by increasing the number of averages for the same total data collection time. Despite current software limitations, the spectra collected in Figs. \ref{fig:CWAp0_Test} were performed on a commercial Bruker E500 instrument with no hardware modifications. Further improvement in segmented NARS is expected by using trapezoidal sweeps and processing both the sweep up and sweep down data. \citep{KITTELL201560, TSEYTLIN2017272}

Applications

In this section, proposed applications are detailed where the SOFFA data collection method will be useful.

Segmented Continuous Wave EPR

A segmented CW EPR experiment processed by the SOFFA method (SOFFA CW) is performed by collecting oversampled data from a standard lock in phase sensitive detector over a fraction of the spectrum and systematically stepping the center field to obtain the whole signal. The field modulation amplitude, time constant, and scan rate can all be adjusted to optimize the oversampled segments.

However, the spectral bandwidth of a CW experiment will always be larger compared to the pure absorption spectral bandwidth due to higher frequency content associated with the derivative like shape from field modulation and phase sensitive detect. When performing a segmented CW experiment, using a large time constant in a phase sensitive detector acts as a low pass filter, which may reduce the effectiveness of the SOFFA filtering. Collecting data with a low time constant and applying the Fourier filter in post processing provides more flexibility.

Field or Frequency Swept Segmented Non-adiabatic Rapid Scan

Field or frequency swept segmented NARS spectroscopy processed by the SOFFA method (SOFFA NARS) is performed by stepping the static magnetic field with a frequency/field sweep smaller than the total spectrum. The step size should be set so significant ($\delta L > 20\text{n}$) overlapping occurs. If sinusoidal sweeps are employed, the more linear 80% of the half wave is used removing 10% of the ends. Further improvement can be obtained with triangular or trapezoidal sweeps. \cite{KITTELL201560}

For NARS spectroscopy, pure absorption is directly collected. Pure absorption has the optimal spectral bandwidth for the SOFFA data acquisition method. In comparison, rapid scan has an increase of spectral bandwidth due to the FID like frequency oscillations and may require over coupling of the resonator to avoid filtering due to the resonator bandwidth.

The implementation of multiple time averaging (MTA) is standard in NARS spectroscopy due to the rapid collection of data at the rate of the field/frequency sweep. \citep{WILMSHURST, MISRARS} MTA is known to filter low frequency and shot noise associated with environmental and physiological noise. Since the data was collected rapidly, such noise is not readily added to the total signal. \citep{WILMSHURST} However, as rates and amplitudes increase, the need to design resonators that exhibit low eddy current forces (vibrational noise) is needed. No change in the collection of a NARS spectrum is needed to implement the SOFFA NARS method.

Frequency Stepped Segmented NMR and MRI

It has become common to use frequency stepping to obtain a broadband \citep{GANDERS201829} or ultra wideband \citep{UltraWideLine} NMR spectrum for exotic \citep{GrandinettiCrystal, MASSIOT1995241, NMRCrystal} and quadrupolar nuclei \citep{OBELL2009330}. Such frequency stepping techniques have also been extended for use with magic angle spinning. \citep{PintaucudaMAS} However, the use of frequency stepping could be configured for narrow band acquisition in order to create a series of spectra that are segmented in frequency. Such a series of frequency stepped segmented NMR spectra could be filtered by the SOFFA method and concatenated.

Conceptually, this can be applied to two dimensional experiments and experiments with gradients, such as MRI.

General Usage

~~Collection of SOFFA data requires the user to be able to step the magnetic field in known quantities (mT) and relate them to a set number of points. The parameters for a traditional CW experiment and SOFFA CW experiment are summarized in Table \ref{table:param}. In modern EPR software (\textit{e.g.}, Bruker XEPR, Bruker MS5000, SpecMan) this is straight forward to calculate from the number of points that are set during configuration. In general, a new sample would require a traditional CW spectrum to be performed to know the full magnetic field width (Sweep Width) of the EPR signal.~~

~~For a SOFFA CW experiment, the user creates a new experimental setup that is separate from the traditional CW experiment. In the example of Fig. \ref{fig:CWApo_Test}, another CW experiment (segment experiment) is chosen on Bruker XEPR and the user sets the spectrometer configuration to start at the lowest magnetic field. In this example, the SOFFA CW segmented sweep width (Seg. Width) is chosen to be a quarter of the total typical CW sweep width (25 mT) and the number of points is set to be 4096. The time constant should be set to the lowest available, since we do not want to pre-filter the data for a SOFFA CW experiment. If desired, the final SOFFA CW signal can be filtered by an RC time constant for comparison to traditional CW.~~

~~In this example, the experimental scan time (30 s) of the segment experiment is set to 1/200th of the total time (including averaging) of the traditional EPR experiment to ensure the SOFFA CW experimental time matches that of the total experimental time of the averaged traditional EPR spectrum. Further averaging of the series of segment experiments that make up a SOFFA CW spectrum is always possible. However, the spectral overlap between segments means that there is already averaging built in (1/40 of 40). Next, the ProDEL file is then loaded into the control and the field step (Seg. Step) is chosen in conjunction with the scan time to match 1/200th of the total field sweep (0.5 mT).~~

~~In the ProDEL code[^]\ref{foot:github}, three variables need to be set. The first is the lowest magnetic field minus one step is placed in 'value', the final magnetic field stop is placed in 'endParValue', and the segment step is placed into the 'parStep' variable. Bruker XEPR then runs the ProDEL script on the active experiment.~~

~~Finally, the data was loaded into the Mathematica script[^]\ref{foot:github} and the appropriate variables are set. The filtering can be adjusted to ensure no broadening occurs (1/50 of 50). Future work will provide a python interface through the Bruker XEPR API to reduce latency and provide real-time filtering capabilities.~~

The total number of points in the final concatenated spectrum $y_{\text{tot}}[i]$ is a function of the oversampling rate, the step size, and the number of steps. To generate a SOFFA spectrum with a conventional number of output points P (for example, 512, 1024, 2048, or 4096), the filtered data are first accumulated onto a high-resolution overlap-add grid and then decimated.

The high-resolution overlap-add grid is constructed at four times the target resolution, with $4P$ evenly spaced points spanning the full field range $[F_{\text{first}}, F_{\text{last}}]$. Each acquired segment $x_{k[j]}$ is mapped onto this grid by computing the field position $f_{k,j} = F_{\text{first}} + k \cdot s + \Delta_j$ for each point j , where Δ_j is the field offset of point j within the segment sweep. The value $x_{k[j]}$ is accumulated into the nearest grid bin and a count is incremented. After all K segments have been processed, each bin is divided by its count to yield the averaged value, and bins with no contributions are filled by linear interpolation from neighboring bins. This accumulation and averaging step is where the segment-overlap averaging takes place on the fine grid.

A filter of variance σ_n^2 is then applied to the high-resolution overlap-add grid by convolution. Finally, the filtered grid is decimated to P output points using a moving-average window, where each output point is the mean of a fixed number of neighboring fine-grid points centered on the corresponding output field position. This produces the final output spectrum $y[p]$, $p = 0, \dots, P-1$. The decimation step conserves the signal-to-noise gains achieved during Fourier block-filtering and segment-overlap averaging. In addition, the moving-average window acts as a final low-pass filter on the fine grid while reducing the number of points to a standard (typically 1024).

Implementation

The block-filtering approach employed by the SOFFA method provides flexibility in filter design. If the filter $H[\omega]$ is constant, as in this work, the output $y[i]$ is equivalent whether block-filtering is used or the oversampled data is filtered after concatenation, but before decimation. One must be careful to always filter before decimation to not reduce the filtering effectiveness. If the filter varies per segment, $H_k[\omega]$, then filtering after concatenation is no longer equivalent.~\citep{OverlapBlock, KARAMI2018209} The SOFFA method therefore splits data processing into two complementary operations: (i) high-frequency filtering and noise shaping, and (ii) low-frequency averaging.

Segmented Continuous-Wave EPR

A SOFFA-CW experiment is performed by collecting oversampled data from a standard lock-in phase-sensitive detector over a fraction of the spectrum and systematically stepping the center field to obtain the full signal. In practice the field modulation amplitude is kept the same as the traditional CW experiment. The number of points is set to 4096 or 8192, time constant is significantly reduced to minimize lock-in noise correlation, and scan rate should be adjusted to optimize the oversampled segments or at the same sweep rate as the traditional experiment. The spectral bandwidth of a CW experiment is larger compared to the partial line shapes acquired with SOFFA allowing for improved filtering of the high frequency noise.

Segmented Non-Adiabatic Rapid Scan

A SOFFA-NARS experiment is performed by stepping the static magnetic field while collecting a field or frequency sweep smaller than the total spectrum width. The step size should be set such that significant overlap occurs ($L > 20n$). For NARS spectroscopy, pure absorption is directly collected, providing the optimal spectral bandwidth for SOFFA. Multiple time averaging (MTA) is standard in NARS due to the rapid data collection rate and filters low-frequency and shot noise associated with environmental sources.~\citep{Wilmshurst, misrARS} No change in the NARS collection procedure is required to implement SOFFA-NARS.

Frequency-Stepped NMR

Frequency stepping is used to obtain broadband~\citep{SANDERS201829} or ultra-wideband~\citep{UltraWideline} NMR spectra for exotic~\citep{GrandinettiCrystal, MASSIOT1995241, NMRCrystal} and quadrupolar nuclei~\citep{ODELL2009330} including applications with magic-angle spinning~\citep{PintacudaMAS} A narrow-band variant of this approach, in which the frequency is stepped to produce a series of segmented spectra, is compatible with the SOFFA method.

\subsubsection{General Usage and Parameter Selection}

Collection of SOFFA data requires the ability to step one parameter in known increments and relate them to a fixed number of points per segment and that the signal of interest is stationary and repeatable in that parameter. Table~\ref{table:param} compares the parameters for a conventional EPR CW experiment and a SOFFA-CW experiment. A traditional CW spectrum should first be collected to determine the full magnetic field sweep width of the EPR signal. In modern EPR software (e.g., Bruker XEPR, Bruker MS5000, SpecMan), the required parameters are straightforward to derive from the configured number of points.

For a SOFFA-CW experiment, a separate experimental configuration is created starting at the lowest magnetic field. In the example of Fig.~\ref{fig:CWAp0_Test}, the SOFFA-CW segment sweep width is set to one quarter of the total sweep (25-mT) with 4096 points per segment. The time constant should be set to the minimum available value to avoid pre-filtering within each segment. The experimental scan time per segment (30~s) is set to $1/200$ th of the total CW experiment time to match the total SOFFA-CW acquisition time. Further averaging of the full SOFFA-CW dataset is always possible; however, the overlap between segments already provides built-in averaging (overlap $m=48$ in this example).

In the ProDEL code\footref{foot:github}, three variables need to be set: the starting field (one step below the lowest field) is placed in \texttt{value}, the final field is placed in \texttt{endParValue}, and the segment step is placed in \texttt{parStep}. Bruker XEPR then executes the ProDEL script on the active experiment. The data is saved by XEPR and the acquired segments are loaded into the Python GUI\footref{foot:github} and the filter variance is adjusted to ensure no spectral broadening.

\begin{table}[htb]

\caption{Comparison of parameters required for a traditional CW experiment and a SOFFA-CW experiment. The traditional time constant (RC filter) should be set as low as possible with SOFFA-CW. Total scan times do not take into account overhead (~~\textit{e.g.}, field flyback time, program lagging, etc.~~)

\caption{Comparison of parameters required for a traditional CW experiment and a SOFFA-CW experiment. The traditional time constant (RC filter) should be set as low as possible for SOFFA-CW. Total scan times do not include overhead (e.g., field flyback time, program latency).}

\centering

\begin{tabular}{l|cc}

@@ -415,8 +352,8 @@

Scan Time (τ) & 240~s & 30~s \\

Aves. & 25 & 1 \\

~~Time Constant & 58.59 ms & -- \\~~

~~Filter (σ) & -- & 50 \\~~

~~Seg. Width (Δ) & -- & 25 mT \\~~

~~Seg. Step (Δ) & -- & 0.5 mT \\ \hline~~

Time Constant & 58.59 ms & -- \\

Filter (σ) & -- & 50 \\

Seg. Width (Δ) & -- & 25~mT \\

Seg. Step (Δ) & -- & 0.5~mT \\ \hline

Total Exp. Time & $t_{\text{Aves.}} \times \tau$ & $t_{\text{Scan}} \times \tau$ \\

& 6000~s & 6000~s

@@ -424,23 +361,78 @@

\end{table}

The SOFFA method is equally applicable to spectra with well-resolved, narrow hyperfine lines. Three parameters govern performance in this regime. First, the Gaussian filter variance σ^2 must be minimized relative to the intrinsic linewidth to prevent spectral broadening. Second, the field step size Δ can be reduced to increase the overlap factor m and thus the number of averaged segments; on the Bruker E500, Δ is practically limited to 0.01~mT and conservatively to 0.025~mT by the field controller precision and magnet hysteresis. Fine adjustment of the effective averaging is therefore most conveniently achieved by varying Δ , while larger gains are better obtained by repeating the full segment stack (repetitions). Third, the per-segment scan rate should not exceed the effective rate of a conventional full-sweep experiment: for example, a 10~mT sweep collected over 60~s implies that each 2~mT segment should require at least 12~s.

\section{Results and Discussion}

The following experiments were tested using the SOFFA method described above.

\subsection{Continuous-Wave EPR}

A series of CW EPR spectra of \textit{apo} [FeFe]-hydrogenase from \textit{Chlamydomonas reinhardtii} of varying concentrations were collected using a bismuth germanate (Bi₄(GeO₄)₃, BGO) dielectric resonator retrofitted in a Bruker MD5 housing~\citep{IVANOV201683} The \textit{apo} protein has one reduced [4Fe-4S]⁺ cluster with an effective $S=1/2$. Three concentrations of 1~mM, 100~ μ M, and 10~ μ M were prepared and confirmed with UV-VIS by measuring the characteristic 400-nm feature indicating relative amounts of [4Fe-4S]~\citep{Knorzer06012012} The conventional-CW spectra were collected by a 4 minute scan of 4096 points over 100~mT. The 1~mM concentration spectrum, shown in Fig.~\ref{fig:CWAp0_Test}A spectrum \textit{i} is intended to be used as a reference. Both the 100~ μ M and 10~ μ M concentrations were collected with 25 averages for a total time of 100 minutes, shown in Fig.~\ref{fig:CWAp0_Test}A spectrum \textit{ii} and \textit{iii}, respectively. Both CW spectra were background subtracted to remove background from the shield.

All CW data was filtered with a $\sigma_n=75$. The 100- μM CW spectrum yielded a signal-to-noise of 181.8, while the SNR of the 10- μM CW spectrum was calculated at 16.5. A SOFFA-CW EPR spectrum was obtained by stepping the field 0.5-mT over 100-mT resulting in 200 steps of 25-mT sweep width (4096 points each). Each segment was collected over 30-seconds for a total time of 100 minutes. A signal-to-noise improvement of 6.1 (1114:181.8) is exhibited between the 100- μM CW experiment and the SOFFA-CW experiment. The SOFFA-CW experiment with 10- μM concentration was also collected in 0.5-mT steps of 25-mT sweep width over 30-s and 4096 points for a total time of 100 minutes. A total of 200-steps were collected over a 100-mT total sweep. The signal-to-noise ratio was calculated to be 83.8 and a signal-to-noise improvement of 5.1 (83.8:16.5) is exhibited for an average of 5.6 increase in concentration sensitivity. All SOFFA-CW spectra were block filtered with a $\sigma=50$ and with an $m=48$. The EPR feature at 340-mT (\ast) is a background caused by residual sodium dithionite which is used to reduce the iron sulfur clusters of the $\text{[FeFe]-hydrogenase}$.

```
\begin{figure}[htbp]
\begin{center}
\includegraphics{05-APO_CW.eps}
\caption{CW spectra were collected on an Bruker E5180 X-band bridge with a dielectric resonator (9.70-GHz) of the reduced  $[\text{Fe}_4\text{S}_4]^{+2}$  of  $\text{[FeFe]-hydrogenase}$  from  $\text{Chlamydomonas reinhardtii}$  at 1-mM, 100- $\mu\text{M}$ , and 10- $\mu\text{M}$  concentrations, spectrum  $\textit{i}$ ,  $\textit{ii}$ , and  $\textit{iii}$ , respectively. The reference spectrum of 1-mM concentration was collected over 100-mT, 4 minute scans averaged 9 times with 4096 points. The traditional CW experiment with 100- $\mu\text{M}$  concentration was collected over 100-mT, 4 minute scans averaged 25 times with 4096 points for a total time of 100 minutes. Both CW spectra were filtered with a  $\sigma_n=75$ . The SOFFA-CW experiment with 100- $\mu\text{M}$  concentration was collected in 0.5-mT steps of 25-mT over 30-s and 4096 points for a total time of 100 minutes. The SOFFA-CW experiment with 10- $\mu\text{M}$  concentration was collected in 0.5-mT steps of 25-mT over 30-s and 4096 points for a total time of 100 minutes. For both SOFFA-CW experiments, a total of 200-steps were collected over a 100-mT total sweep. All segments were block filtered with a  $\sigma=50$  and with an  $m=48$ . All spectra were collected at a temperature of 15-K and at an incident power of 0.63-mW with a field modulation amplitude of 0.5-mT. The EPR feature at 340-mT ( $\ast$ ) is a background caused by residual sodium dithionite which is used to reduce the iron sulfur clusters of the  $\text{[FeFe]-hydrogenase}$ . }
\label{fig:CWApo_Test}
\end{center}
\end{figure}
```

\subsection{Non-adiabatic and Adiabatic Rapid Scan}

```
\begin{figure}[htbp]
\begin{center}
\includegraphics{06-150uM_Heme.eps}
\caption{A 150- $\mu\text{M}$  site-directed spin-labeled Hemoglobin sample in 82% glycerol at 18 $^{\circ}\text{C}$  is collected with conventional-CW EPR in a five-loop--four-gap loop-gap resonator at X-band (9.81-GHz) using 0.1-mT field modulation at a rate of 100-kHz, 5-ms time constant, 16 averages over 20-mT (2-min scan) at 1-mW of microwave power yielding a signal-to-noise of 9.9. A Gaussian filter is applied to the CW data yielding a signal-to-noise of 46.9. SOFFA-NARS data is collected with 0.025-mT steps ( $s$ ) an overlap of  $m=40$  using a trapezoidal field ramp of 11.33-kHz with a 50- $\mu\text{s}$  flat region and an amplitude of 0.5-mT. Data were acquired over 95% of the trapezoidal sweep in one direction. Processing the data with the SOFFA method results in a signal-to-noise of the pure-absorption signal (not shown) of 3890. An MDIFF pseudo-modulation of 0.1-mT field modulation equivalent was used to display the spectrum in a more conventional form, yielding a signal-to-noise of 483.3. The zoomed inset is the first 500 points of the NARS signal. Data was collected on a custom-built X-band bridge dedicated to segmented-NARS spectroscopy. A NARS dispersion signal was also collected (not shown). Both experiments took approximately 32 minutes each.}
\label{fig:150uMHeme}
\end{center}
\end{figure}
```

Conventional CW data is compared to SOFFA-NARS of a 150- μM of a site-directed spin-labeled Hemoglobin sample in 82% glycerol (18 $^{\circ}\text{C}$) at X-band (9.81-GHz), shown in Fig.~\ref{fig:150uMHeme}. Experimental parameters are stated in the figure caption. This sample is in the slow tumbling regime of approximately 15×10^{-9} seconds rotational correlation time τ_{corr} . After 16 averages of 2-min scans a CW signal-to-noise of 9.9 is realized. Adding a Gaussian filter increases the signal-to-noise by a factor of 4.7 (46.9:9.9). By processing the segmented-NARS data with the SOFFA filtering method, the collected pure-absorption signal has a signal-to-noise of 3890 (data omitted). In order to display the spectrum in a more conventional form, the first derivative is computed using an MDIFF pseudo-modulation of 0.1-mT. A signal-to-noise increase of 10.3 (483.3:46.9 compared to the filtered CW data) was achieved for the same measurement time of 32 minutes. The zoomed inset is the first 500 points of the NARS signal multiplied by a factor of 50. Since NARS uses a balanced mixer and A/D converter, the dispersion signal was also collected for no increase in measurement time (data omitted). The NARS linear background was baseline corrected in Xepr.

\subsection{Practical Considerations}

The signal-to-noise ratio of EPR is fundamental to the usefulness of the technique. Improvements in EPR fall into two categories: technical developments, such as resonator and spectrometer advances, multiharmonic data collection\citep{Yu2015may} and advanced averaging and filtering techniques, such as, wavelet analysis\citep{FreedIEEE} and adaptive averaging\citep{COCHRANE200817, Manning2020} techniques. One must take care that any new method does not over-filter and deliver a distorted EPR spectrum.

In addition, the evaluation of new technology must be done with both random Gaussian noise and correlated 1/f noise under consideration. As describe earlier, Gaussian noise is characterized by the uniform power spectral density in the whole frequency space, plotted in Fig.~\ref{fig:ShapeNoise}B(vi). Correlated noise ('Pink' noise), as shown in Figure~\ref{fig:ShapeNoise}(v), where a significant portion of the power spectral density

is located in low frequencies ($1/f$) that overlap with the power spectral density of the EPR signal. It is important to note that 'Pink' noise power spectral density is a function of scan time and can be thought of as a measurement of system stability.~\citep{KITTELL2011228} Because of this, changing the sweep speed changes the correlated noise of the system.

In this experiment, the ^{13}C lines of 10- μM TEMPO have been highlighted by using traditional averaging, shown in black, by scanning 400 times over a 273 minute time period for an SNR of 1146. In contrast, the same signal-to-noise ratio can be achieved in only 20 minutes (red) without loss of the subtle ^{13}C lines by using the SOFFA-CW method for an SNR of 1218.

\begin{figure}[!htb]

\begin{center}

\includegraphics{08-PhaseNoise.eps}

\caption{A 10- μM TEMPO spectrum is recorded using A) traditional CW averaging for 273 minutes (400 averages; black) and using SOFFA-CW in 20 minutes (red). One ^{13}C feature is highlighted. The continuous wave experiment was collected with 10-mT sweep of 1024 points over 41.94 seconds with 400 averages, 20.48-ms time constant, at 3.2-mW, 0.1-mT field modulation at 100-kHz for an SNR of 1146. SOFFA-CW was performed with 3-mT sweep of 8192 points over 10.39 seconds, with 100 steps of 0.1-mT each, 1.28-ms time constant, at 3.2-mW, 0.1-mT field modulation at 100-kHz for an SNR of 1218. B) Phase noise was averaged for 400 averages and added to the continuous wave data (black; SNR of 205) and phase noise was added onto each of the 100 steps of the SOFFA-CW (red; SNR of 768).}

\label{fig:PhaseNoise}

\end{center}

\end{figure}

Since the power spectral density of $1/f$ noise is similar to the EPR signal, both correlated noise and EPR signal have similar shape in the field domain making fitting subtle spectral features difficult without significantly improving the signal-to-noise ratio of the EPR signal with hardware improvements since excessively long averaging will not average out $1/f$ noise.

To definitively isolate the algorithm's performance under strictly controlled $1/f$ drift conditions, a hybrid empirical-simulated approach was utilized. Specifically, the empirically acquired EPR spectra shown in Fig.~\ref{fig:PhaseNoise}A were corrupted by mathematically injecting randomly generated $1/f$ noise into the signal. The noise was implemented in the frequency domain following a $1/f$ power law, establishing a crucial framework for realistic noise modeling in EPR experiments through a systematic process of creating frequency spectra, scaling amplitudes inversely with frequency, and adding random phase components. The implementation maintains mathematical rigor by ensuring conjugate symmetry in the frequency domain, a necessary condition for reconstructing physically meaningful real signals when transforming back to the field domain. The resulting spectrum for continuous wave is shown in black in Fig.~\ref{fig:PhaseNoise}B.

For SOFFA, the randomly generated correlated noise was added to each of the 100 segments and averaging was performed through the SOFFA algorithm. Since the continuous wave EPR experiment and the SOFFA-CW experiment have different sweep times (41.49-s and 10.39-s, respectively) the frequency content of the correlated noise is different and it taken into account in this experiment. The resulting spectrum for SOFFA-CW is shown in red in Fig.~\ref{fig:PhaseNoise}B. From this, it is clear that the subtle ^{13}C lines of the 10- μM TEMPO are lost in the continuous wave EPR spectrum and remain in the SOFFA-CW due to the reduction of SNR from 1146 to 205 when $1/f$ noise was added. The SOFFA method demonstrates enhanced EPR spectral features by not only enhancing the signal-to-noise ratio by a factor of 3.7 compared to traditional continuous wave measurements (767:205), but also effectively mitigating phase noise and $1/f$ correlated noise, thereby preserving subtle spectral features such as ^{13}C lines and enabling more reliable spectral fitting even in challenging low-concentration samples where phase noise starts to dominate due to averaging requirements. Finally, the version of Bruker Xepr (v.2.6b-160) used to collect the SOFFA spectra is not optimized for segmented data acquisition. Future work will implement segmented-NARS using the Xepr Python API interface to decrease the latency associated with large datasets. A signal-to-noise improvement is expected by increasing the number of averages for the same total data-collection time. Despite current software limitations, the spectra collected in Figs.~\ref{fig:CWApo_Test} were performed on a commercial Bruker E580 instrument with no hardware modifications. Further improvement in segmented-NARS is expected by using trapezoidal sweeps and processing both the sweep-up and sweep-down data.~\citep{KITTELL201568, TSEYTLIN2017272}

\conclusions %% \conclusions[modified heading if necessary]

~~The SOFFA data acquisition method, introduced herein for segmented magnetic resonance spectroscopy, has been shown to decrease low frequency background signals and improve the signal to noise ratio by a potential order of magnitude by effectively splitting high frequency filtering with low frequency averaging.~~

~~The use of the block filtering approach employed by the SOFFA method provides a flexible framework for implementing complex filter designs. For example, frequency content could be analyzed and an appropriate filter could be chosen block wise ($S_{H_k}(\omega)$ where $k=0,1,\dots,K$; illustrated in Fig.~\ref{fig:schemes}) to maximize signal to noise while minimizing spectral broadening. Future work studying the effects of adaptive filtering and 'spectral sensing' is underway in order to choose filter parameters without \textit{a priori} information.~\citep{KARAMI2018209, NguyenThanh2013} Additionally, the SOFFA method lends itself to more advanced techniques, such as Wavelet analysis and filtering~\citep{FreedIEEE} or subband multirate filtering~\citep{multirate}, which may yield improved signal to noise and can be customized with \textit{a priori} or real time iterative calculation of the frequency content of the spectrum. Combining advanced filtering techniques with adaptive averaging~\citep{COCHRANE200817, MOVINGADAPT, Manning2020} of the overlapping segments provides a powerful state of the art digital signal processing toolkit for segmented spectroscopy. The SOFFA algorithm also lends itself to multi harmonic detection.~\cite{Hydel1990, Tseitlin2011}~~

~~Current studies using NARS and RS show spectral broadening due to edge effects of the applied sweeping field. In this work, the segment length ΔL was kept small to remain in the more linear portion of the sinusoidal sweep, thus negating this effect. However, this spectral broadening limits the size of ΔL . This challenge~~

can be addressed by using a trapezoidal sweep where the segments are collected during the linear rise or falloff of the field/frequency sweep and the plateau is longer than the relaxation time of the spin system. This setup would minimize edge effects caused by abrupt changes of a triangular sweep or turning points of a sinusoidal sweep. Potentially, for RS, deconvolution of each segment block-wise before filtering is feasible. Future work will explore these possibilities.

It should be noted that the first field-stepped RS spectra were obtained by Eaton and colleagues. \citep{YU201558} However, segmented RS differs from the enabling field-stepped RS spectra described therein. The work of Ref. \citep{YU201558} stepped the field while the whole RS spectrum was excited and then averaged together. In future work, the field can be stepped from an off resonance position through the EPR signal and again to off resonance just as it is performed with SOFFA NARS.

As frequency-swept NARS and RS are more widely adopted, the SOFFA filtering technique introduced here may provide additional benefit by filtering and averaging signals from the frequency response of microwave components which create large and often quadratic backgrounds. \citep{HYDE201093, TSEITLIN2011156, Strangeway2017} By using the first frequency or field sweep in the NARS data collection, the large static frequency response can be background subtracted from the whole dataset before processing.

By implementing SOFFA CW on a standard Bruker E500 spectrometer and collecting segmented CW is straight forward and demonstrates an increase in concentration sensitivity of 6.9 for the same measurement time. In a SOFFA NARS experiment, a factor of 10.3 signal to noise improvement, shown in Fig. \ref{fig:150uMHeme}, is achieved with no change in the experimental procedure described in the literature. \citep{KITTELL2011228, HYDE201315, KITTELL201568}

Finally, the SOFFA method is also useful for real-time segmented NARS processing, since the Fourier block-filtering can be easily parallelized on modern computers and displayed as the data are collected. As the SOFFA method matures, advanced filtering techniques may provide significant improvements over traditional overlap-add averaging. \citep{COCHRANE200817, MOVINGvADAPT, Manning2020}

The SOFFA data acquisition method, introduced herein for segmented magnetic resonance spectroscopy, has been shown to decrease low-frequency background signals and significantly improve the signal-to-noise ratio by effectively splitting high frequency filtering with low frequency averaging.

The improvements described here are phenomenological: the SOFFA method is built upon known DSP foundations, and the signal-to-noise gains are demonstrated experimentally rather than derived from a unified analytical model. A quantitative first-principles treatment (one that predicts the net SNR improvement as an explicit function of overlap factor \mathcal{M} , oversampling ratio OSR, filter variance σ_n^2 , and noise color) is the subject of ongoing work. Nevertheless, the experimental data presented across three distinct EPR measurement conditions consistently demonstrates the practical value of the approach across biologically relevant samples and measurement conditions. The ProDEL script and Python GUI are publicly available to facilitate adoption. \footref{foot:github}

The use of the block-filtering approach employed by the SOFFA method provides a flexible framework for implementing complex filter designs. For example, frequency content could be analyzed and an appropriate filter could be chosen block-wise ($\mathcal{H}_k(\omega)$ where $k=0,1,\dots,K$; illustrated in Fig. \ref{fig:schemes}) to maximize signal-to-noise while minimizing spectral broadening. Future work studying the effects of adaptive filtering and "spectral sensing" is underway in order to choose filter parameters without \textit{a priori} information. \citep{KARAMI2018209, NguyenThanh2013} Additionally, the SOFFA method lends itself to more advanced techniques, such as Wavelet analysis and filtering \citep{FreedIEEE} or subband-multirate filtering \citep{multirate}, which may yield improved signal-to-noise and can be customized with \textit{a priori} or real-time iterative calculation of the frequency content of the spectrum. Combining advanced filtering techniques with adaptive averaging \citep{COCHRANE200817, MOVINGvADAPT, Manning2020} of the overlapping segments provides a powerful state-of-the-art digital signal processing toolkit for segmented spectroscopy. The SOFFA algorithm also lends itself to multi-harmonic detection. \citep{Hyde1990, Tseitlin2011}

Current studies using NARS show spectral broadening due to edge effects of the applied sweeping field. In this work, a trapezoidal sweep was used and 95% of the linear portion was collected, thus minimizing this effect. This spectral broadening limits the size of ΔL . The challenge can be further addressed by using a trapezoidal sweep where the plateau is longer than the relaxation time of the spin system, allowing the segments to be collected entirely during the flat region. This setup would minimize edge effects caused by abrupt changes of a triangular sweep or turning points of a sinusoidal sweep.

It should be noted that the first field-stepped RS spectra were obtained by Eaton and colleagues. \citep{YU201558} However, segmented-RS differs from the enabling field-stepped RS spectra described therein. The work of Ref. \citep{YU201558} stepped the field while the whole RS spectrum was excited and then averaged together. Potentially, for rapid scan, deconvolution of each segment block-wise before filtering is feasible. \citep{TSEITLIN2017272} Future work will explore these possibilities.

As frequency-swept NARS and RS are more widely adopted, the SOFFA filtering technique introduced here may provide additional benefit by filtering and averaging signals from the frequency response of microwave components which create large and often quadratic backgrounds. \citep{HYDE201093, TSEITLIN2011156, Strangeway2017} By using the off resonance frequency- or field-sweep in the NARS data collection, the large static frequency response can be background subtracted from the whole dataset before processing without adding significant overhead.

Implementing SOFFA-CW on a standard Bruker E500 spectrometer and collecting segmented CW is straight-forward and demonstrates an increase in concentration sensitivity of 6.9 for the same measurement time. In a SOFFA-NARS experiment, a factor of 10.3 signal-to-noise improvement, shown in Fig. \ref{fig:150uMHeme}, is achieved with no change in the experimental procedure described in the literature. \citep{KITTELL2011228, HYDE201315, KITTELL201568}

Finally, the SOFFA method is also useful for real-time segmented-NARS processing, since the Fourier block-filtering can be easily parallelized on modern computers and displayed as the data is collected. As the SOFFA method matures, advanced filtering techniques may provide significant improvements over traditional

```
overlap-add averaging. \citep{COCHRANE200817, MOVINGvADAPT, Manning2020}
```

```
%% The following commands are for the statements about the availability of data sets and/or software code corresponding to the manuscript.
```

```
%% It is strongly recommended to make use of these sections in case data sets and/or software code have been part of your research the article is based on.
```

```
\codedataavailability{Code and data are available upon request.} %% use this section when having data sets and software code available
```

```
\codedataavailability{The ProDEL script and Python GUI used to collect and process SOFFA data are available at \url{https://github.com/jsidabras/SOFFABruker}.} %% use this section when having data sets and software code available
```

```
\appendix
```

```
@@ -448,5 +440,5 @@
```

```
\renewcommand{\thefigure}{A\arabic{figure}}
```

```
\section{Shape of Noise}
```

Plots of simulated Gaussian spectra in field and Fourier space, Figs.~\ref{fig:ShapeNoise}A and ~\ref{fig:ShapeNoise}B, respectively. A noiseless Gaussian is shown in Fig.~\ref{fig:ShapeNoise} spectrum \textit{i} and white noise is added to make the signal-to-noise approximately 4, shown in Fig.~\ref{fig:ShapeNoise} spectrum \textit{ii}. By filtering the noisy spectrum with a Gaussian filter (Fig.~\ref{fig:ShapeNoise}B; dashed-line) the noise outside of the spectral bandwidth (f_{cw}) can be removed, shown in Fig.~\ref{fig:ShapeNoise} spectrum \textit{iv}. However, by oversampling, shown in Fig.~\ref{fig:ShapeNoise} spectrum \textit{iii}, the spectral bandwidth is reduced (f_{s}) by the oversampling factor OSF and the noise power spectral density is reduced by the same amount. In order to mimic the methodology of oversampled segmented-data collection, the number of points remain the same, but the collected data ~~are~~ only a segment with a quarter of the field sweep.

Plots of simulated Gaussian spectra in field and Fourier space, Figs.~\ref{fig:ShapeNoise}A and ~\ref{fig:ShapeNoise}B, respectively. A noiseless Gaussian is shown in Fig.~\ref{fig:ShapeNoise} spectrum \textit{i} and white noise is added to make the signal-to-noise approximately 4, shown in Fig.~\ref{fig:ShapeNoise} spectrum \textit{ii}. By filtering the noisy spectrum with a Gaussian filter (Fig.~\ref{fig:ShapeNoise}B; dashed-line) the noise outside of the spectral bandwidth (f_{cw}) can be removed, shown in Fig.~\ref{fig:ShapeNoise} spectrum \textit{iv}. However, by oversampling, shown in Fig.~\ref{fig:ShapeNoise} spectrum \textit{iii}, the spectral bandwidth is reduced (f_{s}) by the oversampling factor OSF and the noise power spectral density is reduced by the same amount. In order to mimic the methodology of oversampled segmented-data collection, the number of points remain the same, but the collected data **is** only a segment with a quarter of the field sweep.

An example of pink noise is shown in Fig.~\ref{fig:ShapeNoise} spectrum \textit{v}. The power spectral density, shown in Fig.~\ref{fig:ShapeNoise}B illustrates the challenge with filtering pink noise: the concentration of power spectral density in the same region of the spectral bandwidth. Whereas white noise, shown in Fig.~\ref{fig:ShapeNoise} spectrum \textit{vi}, has a flat power spectral density response.

```
@@ -461,17 +453,4 @@
```

```
\appendixfigures %% needs to be added in front of appendix figures
```

```
\end{figure}
```

```
\setcounter{figure}{0}
```

```
\renewcommand{\thefigure}{B\arabic{figure}}
```

```
\section{Variable Definitions}
```

~~The nomenclature of the Welch FFT procedure for power spectral density is adopted, due to the similarity of segmentation of a discretized signal. The variables used in this work are outlined in~~

~~Fig. \ref{fig:Variables}. \citep{WelchFFT}~~

```
\begin{figure}[htbp]
```

```
\begin{center}
```

```
\includegraphics{S2 Variables.eps}
```

```
\caption{Illustration of spectral segmentation with parameters and variables.}
```

```
\label{fig:Variables}
```

```
\end{center}
```

```
\end{figure}
```

```
\noappendix %% use this to mark the end of the appendix section. Otherwise the figures might be numbered incorrectly (e.g. 10 instead of 1).
```